BATTERY CHARGE CONTROL FOR STANDALONE PV SYSTEM BY USING MATLAB/SIMULINK

Afnan Waleed SAFFAR

2021
MASTER THESIS
ELECTRICAL-ELECTRONICS ENGINEERING

Thesis Advisor
Assist. Prof. Dr. Ersagun Kürşat YAYLACI

BATTERY CHARGE CONTROL FOR STANDALONE PV SYSTEM BY USING MATLAB/SIMULINK

Afnan Waleed SAFFAR

T.C.
Karabuk University
Institute of Graduate Programs
Department of Electrical-Electronics Engineering
Prepared as
Master Thesis

Thesis Advisor
Assist. Prof. Dr. Ersagun Kürşat YAYLACI

KARABUK
August 2021

I certify that in my opinion the thesis submitted by Afnan Waleed SAFFAR titled "BATTERY CHARGE CONTROL FOR STAND-ALONE PV SYSTEM BY USING MATLAB\SIMULINK" is fully adequate in scope and in quality as a thesis for the degree of Master of Science.

Assist. Prof. Dr. Ersagun Kürşat YAYLACI .....
Thesis Advisor, Department of Electrical-Electronics Engineering

This thesis is accepted by the examining committee with a unanimous vote in the Department of Electrical-Electronics Engineering as a Master of Science thesis. August 18, 2021

Examining Committee Members (Institutions)	Signature
Chairman : Assoc. Prof. Dr. Selim ÖNCÜ (KBU)	.....
Member : Assist. Prof. Dr. Selçuk EMİROĞLU (SAU)	.....
Member : Assist. Prof. Dr. Ersagun Kürşat YAYLACI (KBU)	.....

The degree of Master of Science by the thesis submitted is approved by the Administrative Board of the Institute of Graduate Programs, Karabuk University.

Prof. Dr. Hasan SOLMAZ .....
Director of the Institute of Graduate Programs

"I declare that all the information within this thesis has been gathered and presented in accordance with academic regulations and ethical principles and I have according to the requirements of these regulations and principles cited all those which do not originate in this work as well."

Afnan Waleed SAFFAR

ABSTRACT

M. Sc. Thesis

BATTERY CHARGE CONTROL FOR STANDALONE PV SYSTEM BY USING MATLAB/SIMULINK

Afnan Waleed SAFFAR

Karabuk University
Institute of Graduate Programs
Department of Electrical-Electronics Engineering

Thesis Advisor:
Assist. Prof. Dr. Ersagun Kürşat YAYLACI
July 2021, 71 pages

Due to the depletion of fossil fuels and their environmental damage, the tendency for renewable energy sources is increasing. Photovoltaic (PV) system is one of the renewable energy sources, and its use is becoming widespread day by day. However, since PV sources are intermittent energy sources, PV systems must be operated with energy storage systems in many areas. Within the scope of this thesis, battery charge control of an autonomous PV system is carried out via a DC-DC Buck converter. A lead-acid (LA) battery, which offers an advantage with its affordable cost, is used as a battery. In addition, for the system to be operated efficiently, it must be operated at the maximum power point (MPP). For this purpose, battery charge control, which can follow the maximum power point, was carried out with the Perturb&Observe (P&O) and Incremental Conductance (IC) methods, widely used in the literature. The methods were applied to the autonomous PV system implemented in MATLAB/Simulink environment with the same step sizes and sampling times. The simulation results were

presented comparatively by considering control criteria such as steady-state error and settling time.

Key Word **:** Stand-alone PV system, DC-DC Buck converter, PID controller, Lead-acid Battery, P&O, IC

Science Code : 90544

ÖZET

Yüksek Lisans Tezi

MATLAB\SİMULİNK KULLANARAK OTONOM PV SİSTEM İÇİN AKÜ ŞARJ KONTROLÜ

Afnan Waleed SAFFAR

Karabük Üniversitesi
Lisansüstü Eğitim Enstitüsü
Elektrik-Elektronik Mühendisliği Anabilim Dalı

Tez Danışmanı:
Dr. Öğr. Üyesi Ersagun Kürşat YAYLACI
Ağustos 2021, 71 Sayfa

Fosil yakıtların tükenmesi ve çevresel zararları sebebiyle yenilenebilir enerji kaynaklarına yönelim artış göstermektedir. Fotovoltaik sistem yenilenebilir enerji kaynaklarından birisi olup her geçen gün kullanımı yaygınlaşmaktadır. Ancak PV kaynakların kesintili bir enerji kaynağı olması sebebiyle birçok alanda PV sistemlerin enerji depolama sistemleri ile çalıştırılması gerekmektedir. Bu tez kapsamında otonom bir PV sisteminin alçaltıcı tip DC-DC dönüştürücü üzerinden batarya şarj kontrolü gerçekleştirilmiştir. Batarya olarak uygun maliyeti ile avantaj sunan kurşun-asit batarya kullanılmıştır. Ayrıca sistemin verimli olarak çalıştırılabilmesi için maksimum güç noktasında işletilmesi gerekmektedir. Bu amaçla literatürde yaygın olarak kullanılan değiştir-gözle (D&G) ve artan iletkenlik (AI) yöntemleri ile maksimum güç noktası takibi yapabilen batarya şarj kontrolü gerçekleştirilmiştir. Yöntemler aynı adım büyüklükleri ve örnekleme zamanları ile MATLAB/Simulink ortamında gerçeklenen otonom PV sistemine sisteme uygulanmış olup simülasyon sonuçları

sürekli-hal hatası, yerleşme zamanı gibi kontrol kriterleri dikkate alınarak karşılaştırmalı olarak sunulmuştur.

Anahtar Sözcükler : Otonom fotovoltaik sistem, alçaltıcı tip DC-DC dönüştürücü, PID denetleyici, kurşun-asit batarya, D&G, AI

Bilim Kodu : 90544

ACKNOWLEDGMENT

It gives me great pleasure to communicate my feelings heartfeltly. I am grateful to my advisor, Assist. Prof. Dr. Ersagun Kürşat YAYLACI, for his counsel and support during this study, I would like to express my utmost gratitude to him for being very understanding and supporting particularly and encouragement along with the entire project since the day I enrolled in the master's program.

I would also like to thank Assoc. Prof. Dr. Selim ÖNCÜ for his valuable guidance throughout my studies. He provided me with the tools that I needed to choose the right direction and successfully complete my dissertation.

To my family who challenges me to be courageous. I am dedicated to them for their continuing love and prayers, as well as for being my pillar of strength, which has helped me overcome all obstacles and problems in finishing this thesis, and to all of my friends for their understanding, support, and collaboration.

CONTENTS

Page

Page

LIST OF FIGURES

Page

Page

LIST OF TABLES

Page

SYMBOLS AND ABBREVITIONS INDEX

SYMBOLS

I_{pv} : photovoltaic panel current

Vpv : photovoltaic panel voltage

V_S : source voltage

I_S : source current

S : switch

D : diode

L : inductance

I_L : inductance current

V_L : inductance voltage

C : output conductance

V_O : output voltage

I_O : output current

R : resistance (load)

R_s : series resistance

R_{sh} : shunt resistance

I_{ph} : photon current

I_{sc} : short-circuit current

V_{oc} : open-circuit voltage

F_s *:* switching frequency

Esr : equivalent series resistance

Ah : amper hour

P_{ext} *: extracted power*

P_{max} *: maximum power*

η_{MPO} *perturb and observe efficiency*

η_{MIC}*: incremental conductance efficiency*

ABBREVITIONS

DC : Direct current

PWM : Pulse width modulation

MPPT : Maximum power point tracking

MPP : Maximum power point

PID : Proportional integral derivation controller

PV : Photovoltaics

DOD : Depth of discharge

SOC : State of charge

P&O : Perturb and observe method

IC : Incremental conductance method

CCM : Contusion's conduction mode

DCM : Discontinuous conduction mode

TWh *:* Terra watt hour

CV : Constant voltage method

VOC : Open voltage method

BMS : Battery management system

Li-ion : Lithium-ion battery

LA : Lead acid battery

PART 1

INTRODUCTION

The technical potential of renewable energy has been projected to be at least 18 times of the present world's primary energy consumption [1]. Increasing energy demand throughout the world, as well as the depletion of fossil energy sources, promote, other energy sources are being investigated, such as fuel cells, solar energy, and other clean energy sources. The majority of these energies are ecologically beneficial [2]. Because renewable technologies are considered clean energy sources, and their best utilization reduces environmental negative consequences[1-3]. Photovoltaic (PV) consists of converting directly radiated light solar into electricity. PV panels made up of solar cells are used to carry out this energy transfer. Thermal solar energy, on the other hand, generates heat from the Sun's infrared radiation in order to heat air, water, and other fluids. When compared to PV technology, this technique is simpler and hence less expensive. It operates based on collecting calories by using heat-absorbing materials like black metal sheets as given in Figure 1.1 [4]. Thermodynamic solar energy, on the other hand, is a technology used in large power plants to heat a fluid to a very high temperature, which is then used to produce steam via thermal exchange and generate electricity via a steam-driven turbine [4].

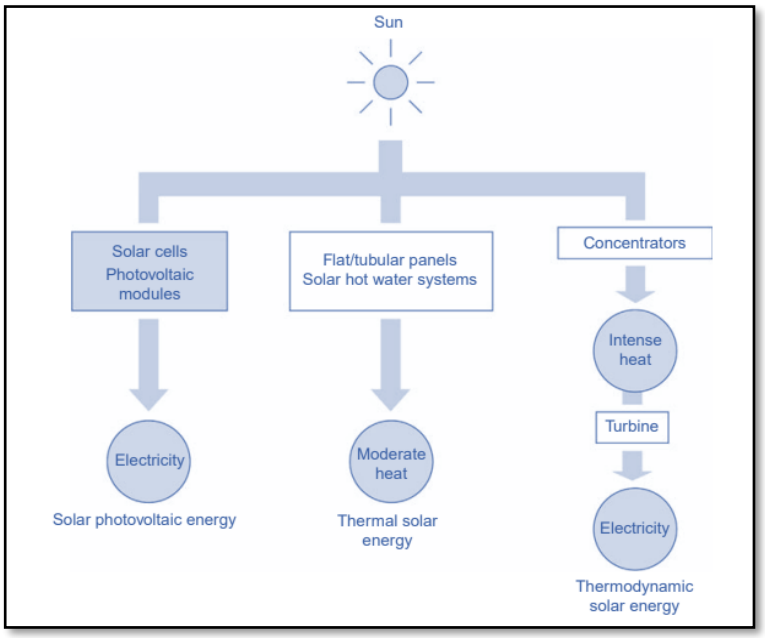

Figure 1.1. Some techniques for utilizing solar energy [2].

1.1. AIM AND OBJECTIVE OF THE THESIS

The energy generated by the PV panels is the primary source of energy in a standalone PV system. Otherwise, a battery is required to keep the acquired energy and provide power delivery at night or during periods of low electrical radiation. The batteries mainly provide the storage of electrical energy. The LA battery is commonly employed in solar systems and automobiles, industrial equipment, and energy storage systems [5]. In this regard, this thesis provides a control approach for a standalone solar system's effective Lead-acid battery. Maximum power point tracking (MPPT) controller algorithms are crucial for getting the most power out of PV panels. As an interface between the solar array and the battery, an MPPT method requires a Buck DC converter. The task of the MPPT is matching the PV current with maximum power point (MPP) to the current of the PV array under changing atmospheric conditions [6].

1.2. LITERATURE REVIEW

Three critical technical developments are generally included in sustainable energy development strategies, energy savings, energy efficiency, and replacing fossil fuels with alternative renewable energy sources [6]. By replacing renewable energy sources with traditional energy sources, renewable energy technologies provide a great potential to minimize global warming and greenhouse gas emissions [4].

Heat and light are the two major types of solar energy. Sunlight and heat are changed and absorbed in several ways by the environment. Further, improvements in the energy efficiency of the solar PV manufacturing process and higher conversion efficiency and longer module lifetimes have received a lot of attention to shorten the energy payback period and minimize greenhouse gas emissions. According to the life cycle assessment approach, monocrystalline silicon has the highest energy consumption, longest energy payback time, and highest greenhouse gas emissions rate compared to other solar PV technologies [1-5].

In [6], the high-level control permits the DC motor's rotational velocity to follow the needed trajectory while also delivering the desired voltage profile for the output voltage of the DC-DC Buck converter. The outcome demonstrates that the required angular velocity is well tracked under the given conditions and even when the system parameters change abruptly.

In [7], MPPT approaches have been described and classified based on characteristics such as the sorts of control strategies utilized and the types of circuits suitable for PV systems, commercial and practical applications.

In [8], a Model Predictive Control (MPC) based MPPT algorithm is used for photovoltaic systems. It is from the results that the offered control technique offers good dynamic performance.

In [9], a novel modified IC variable step size algorithm was established. Experimental results demonstrate high accuracy, quicker convergence speed, and less oscillation

around the MPP. As a consequence, the suggested IC algorithm is more efficient.

In [10], a comparison of Buck versus Boost MPPT topologies is made. Hereof, a variable step size that has been changed of P&O algorithm has been developed, which may concurrently enhance the PV system's dynamic and steady-state performance. Traditional methods have flaws, which the suggested variable step size technique addresses.

In [11], different MPPT methods have been examined and simulated in various irradiation conditions. the simulation results seen that the P&O and IC algorithms have extremely similar performances and dynamic reaction times and that both methods have shortcomings of steady-state oscillation due to perturbations.

In [12], the MPPT performance of P&O and IC algorithms is compared for the convergence time. It is demonstrated that the convergence time is larger for IC.

In [13], a Lead-Acid battery charger is developed. It can also provide the MPPT using the IC algorithm, and the system has a fast dynamic response.

In [14], the accuracy of the MPPT algorithm for locating the maximum power point (MPP) is improved by using the Fuzzy Logic algorithm, which approaches the solar panel.

In [15], the output power of the Buck converter is controlled using a PID controller. The output voltage has a fast dynamic response and is resistant to load and input voltage fluctuations.

In [16], a modified Firefly method to estimate the MPP for PV systems under various illuminations, as the results showed that the better performance in algorithm speed and system efficiency.

In [17], a new MPPT method has been described for PV. In comparison to several existing approaches, the suggested strategy eliminates some necessities, such as a rough approximation of panel output characteristics and complex mathematical calculations.

In [18], MPPT methods are compared, and it is pointed that the variable step-size based P&O method is the best one for the PV systems.

In [19], a modified IC algorithm is designed. The simulation results show that the method is effective for various operating situations while maintaining the best dynamic state performance, decreasing power loss, and increasing tracking efficiency.

In [20], the IC method is used for the solar irradiation level changes. The suggested method has 0% oscillation in power, and fast dynamic performance as the solar irradiation level increases.

New technologies of power electronics are presently being developed to improve the efficiency of electricity and energy regulation. Power electronics are replacing older electro-mechanical and electrical systems in motion control applications due to their higher efficiency and tighter control features [21].

In [22], the IC MPPT algorithm is offered. To link the PV panel with load, a DC-DC converter has been utilized. The offered MPPT algorithm responds rapidly and accurately, and it soon reaches a steady-state.

PART 2

THE CONTROL OF PV SYSTEMS BY THE MPPT METHODS

2.1. PV SYSTEMS

PV system electricity generation in 2011 about 73,745 MW, there has been a significant increase in PV system installation reaching about 713,970 MW at 2020 years [23]. The PV systems can be divided into 2 categories, grid connection and standalone systems. PV feeds the loads directly without connecting to the utility system in standalone systems, which offer the advantage of a simplified system design and control strategy [14]. In the PV panel, the photovoltaic cells create power from sunlight. The primary point to consider is energy conversion efficiency. Regarding the panels, the critical primary point is how the cells are connected since this is decisive for the amount of the generated power [5]. The Solar cells are made of PN junction constructed with a slim frame semiconductor layer. When exposed to light, photons with higher energy than the semiconductor's bandgap energy are absorbed, forming a pair of electron holes. The PN-junction is the fundamental unit of carrier production and recombination in semiconductors, equivalent to an electron transiting between the conduction band and the valence band [19], as shown in Figure 2.1.

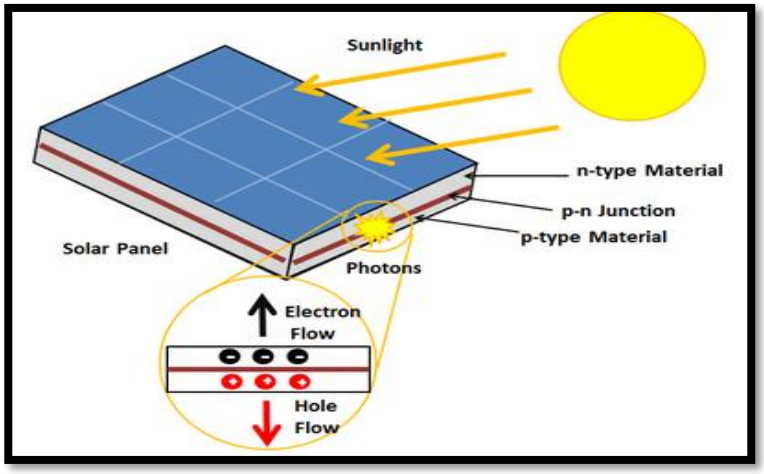

Figure 2.1. A PN junction silicon PV cell [19].

The PV system can be modelled with a current source and a parallel diode, as shown in Figure 2.2. This model is called as a single diode PV cell model.

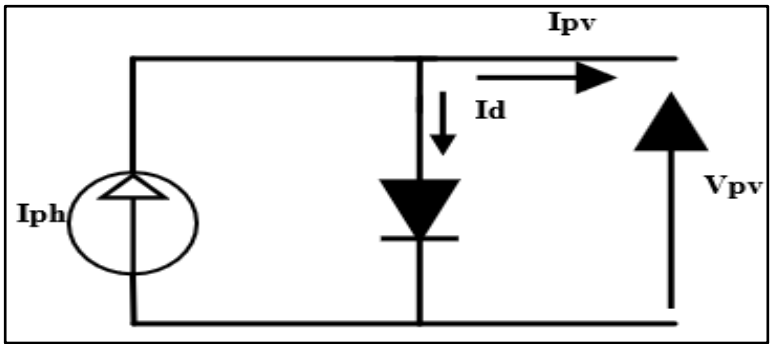

Figure 2.2. Single diode ideal PV cell equivalent model.

The PV current (I_{pv}) is obtained directly from the Kirchhoff law [7]:

$$I_{pv} = I_{ph} - I_d \tag{2.1}$$

where I_{ph} is a photon current (A), I_d is a diode current (A). The diode current is $I_d = I_s(e^{\frac{qVpv}{mkT}} - 1)$ as a consequence, the output current is given by the nonlinear I-V equation below.

$$I_{pv} = I_{ph} - I_s(e^{\frac{qVpv}{mKT}} - 1) \tag{2.2}$$

where V_{pv} is a PV module voltage (V), I_s is a diode current in the reversal of saturation (A), q is the charge of an electron ($1{,}6 * 10^{-19}$ C), k is a Boltzmann's constant, and it is about ($1.38*10^{-23}\frac{J}{k}$), T is the cell temperature, and m= Q_d*N_s, where, Q_d is an ideality factor value of diode, and N_s is the number of cells in series, as given in Figure 2.3. series and shunt resistance, respectively (R_s, R_{sh}). R_{sh} can be neglected in the analysis [24], because it has a large value, as shown in Figure 2.3. The PV current can be deduced directly by using the Kirchhoff law.

$$I_{pv} = I_{ph} - I_d - I_{sh} \tag{2.3}$$

where the diode current is:

$$I_d = I_s \left(e^{\frac{q\,(Vpv + R_S\, Ipv)}{mKT}} - 1 \right)$$

and the shunt current is:

$$I_{sh} = \frac{V_{pv} + R_S I_{pv}}{R_{sh}}$$

The single-diode model predicts which equation governs the relationship between the solar cell output current and shunt current as Equation 2.4 [7].

$$I_{pv} = I_{ph} - I_s \left(e^{\frac{q\,(Vpv + R_S\, Ipv)}{mKT}} - 1 \right) - \frac{V_{pv} + R_S I_{pv}}{R_{sh}} \tag{2.4}$$

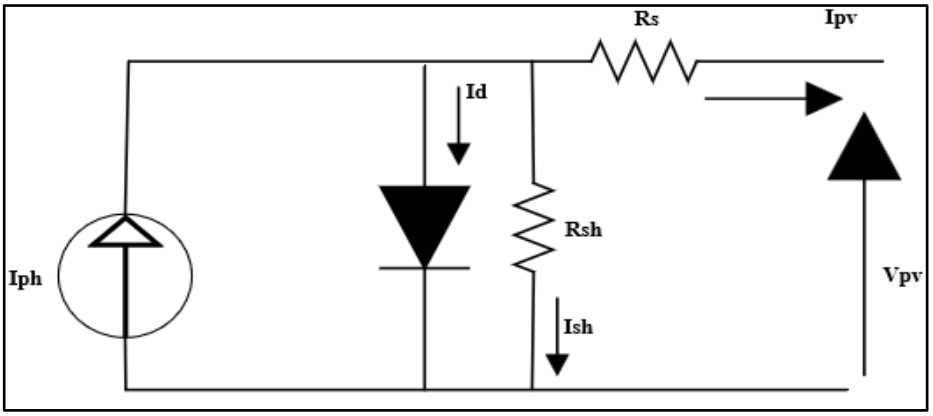

Figure 2.3. A Single diode PV cell equivalent model with shunt and series resistance.

2.2. THE MAXIMUM POWER POINT TRACKING (MPPT) METHODS

In renewable energy applications, PV energy sources are frequently employed [8]. Solar irradiation, temperature, and load current all affect the output voltage, the output current, and the power of a PV array. Such as a result, the impacts of these three factors must be considered when designing PV arrays. MPPT must be accustomed to push the operating point to the MPP of the PV modules for solving this problem. MPPT can retrieve over 97 percent of the PV power which properly optimized [10-12].

The main logic of the MPPT is to correspond the load's impedance to the PV module's impedance [13]. The MPP's position in the PV module's I-V curve is never known in advance, and depending on irradiance and temperature, it varies dynamically. Consequently, the tracking algorithm, which is the MPPT controller's heart, is used to find the MPP [13]. There are many MPPT algorithms in the literature, and some of them related this thesis are presented with subsections as follows.

2.2.1. The P&O Method

The P&O approach is the most popular often used direct MPPT methodology. It is characterized by introducing a tiny disturbance into the system, the consequences of which are utilized to reposition the operational point closer to the MPP [17]. By analyzing real values of current and PV

voltage, the P&O can track the highest power point at all times, regardless of meteorological conditions or kind of PV panel. Because of its ease of implementation and simplicity, the P&O technique is extensively employed in PV systems. However, it has flaws, including sluggish response time, oscillation around the MPP in steady-state, and also even tracking in the wrong direction under quickly varying atmospheric conditions [18].

The principle behind the P&O technique is as follows. The PV operating point is disturbed regularly by altering the current at the control algorithm compares the power produced by the PV source before and after each perturbation. If the PV power increases after the perturbation, the operating point has been shifted closer to the MPP. As a result, the current's following perturbation will have the same sign as the prior one. If the power produced from the PV drops following a current disturbance, the operating point will shift away from the MPP. As a result, the succeeding current perturbation's sign is inverted. The switching converter is used to drive the PV generator's operational current perturbation [17]. The flowchart of the P&O algorithm is given in Figure 2.4.

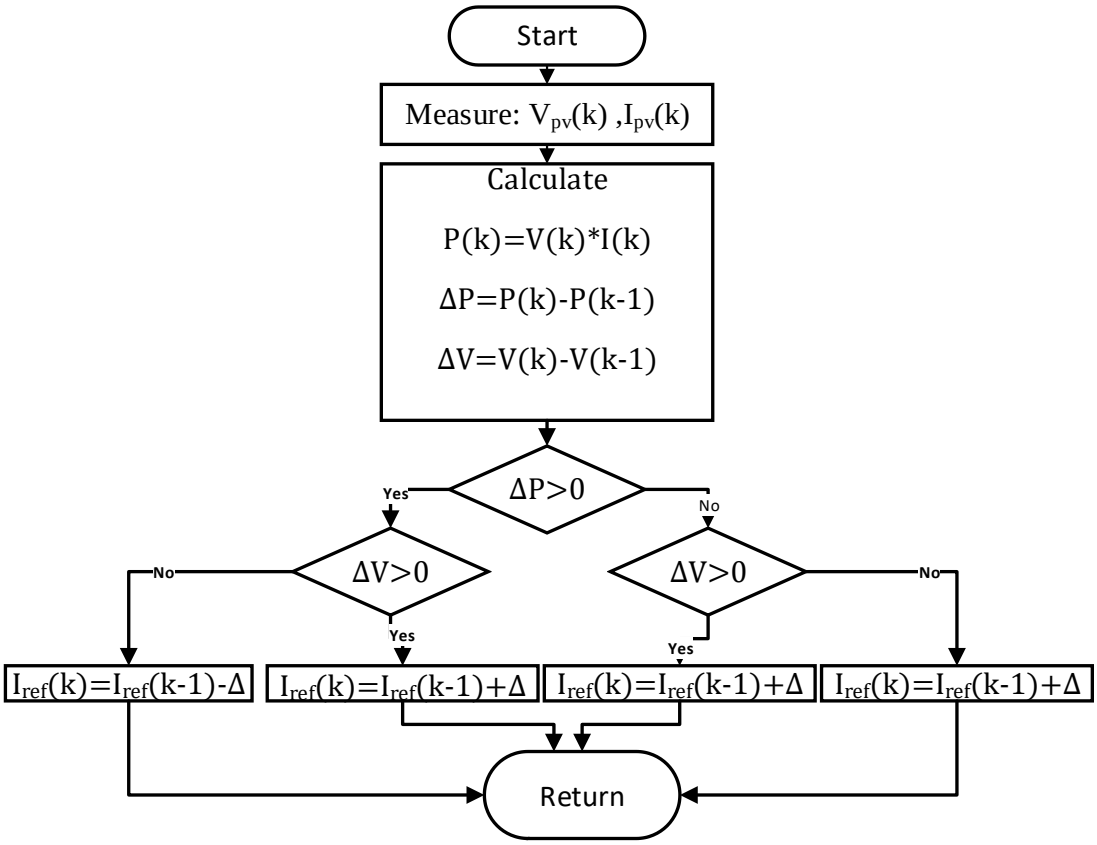

Figure 2.4. The P&O algorithm flowchart.

2.2.1.1. Modified P&O Method

The P&O algorithm can apply a wrong control law to the system when the irradiation changes suddenly. To solve this problem, the modified perturb and observe (MP&O) method is offered. The suggested method is also capable of removing the oscillation that occurs around the MPP. The flowchart of the proposed method is illustrated in Figure 2.5.

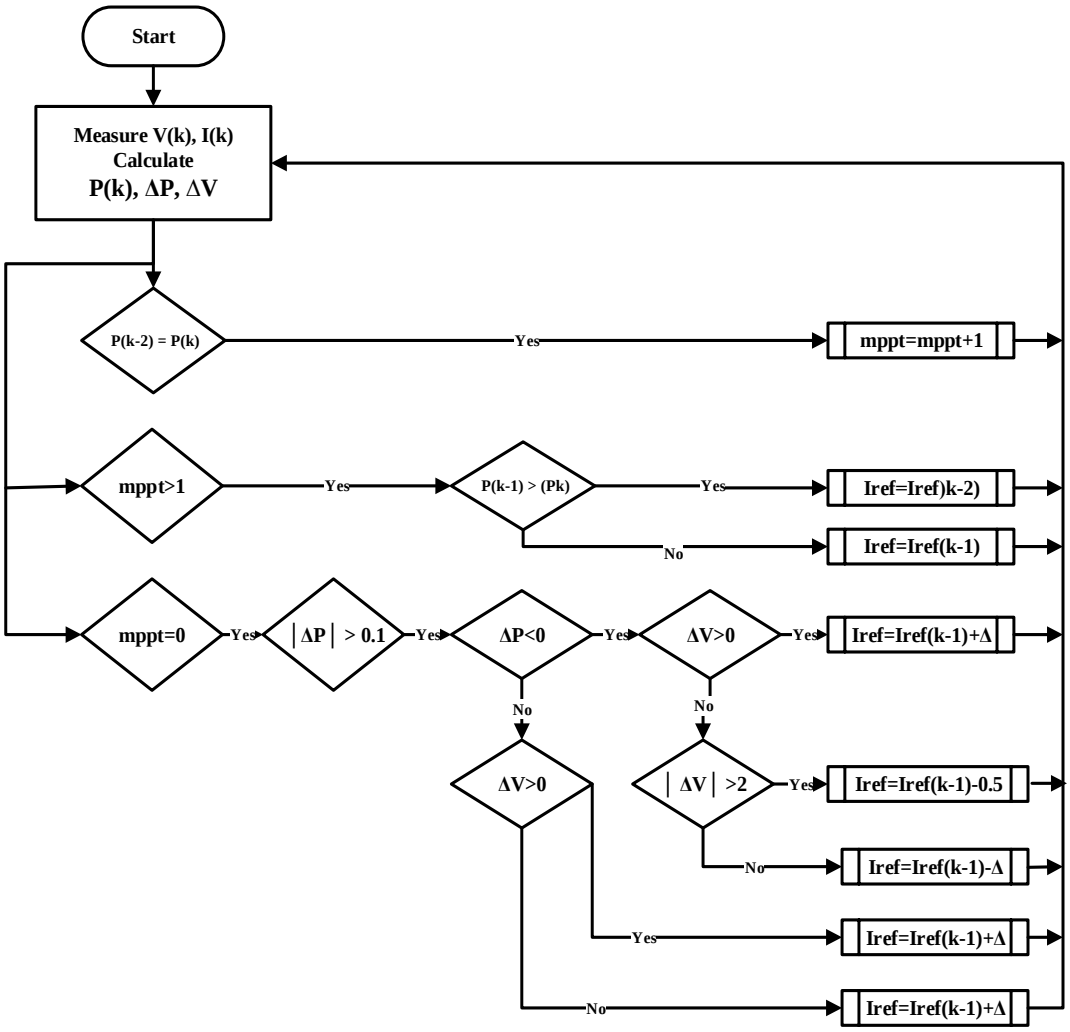

Figure 2.5. The flowchart of MP&O algorithm.

2.2.2. The IC Method

The IC method is based on the slope of the P–V curve, which is influenced by the amount of solar irradiation. As the algorithm uses the current or voltage of the PV module in the calculation, the effect of solar irradiation and load changes on the current and voltage of the PV module must be considered in the algorithm [25]. Table 2.1 shows the position of the operating voltage of the system concerning .the slope in the incremental conductance method. The flowchart of the IC algorithm is given in Figure 2.6.

Table 2.1. Determination of incremental conductance method.

Slope	**System operating voltage**
$\frac{dP}{dV} = 0$	At MPP
$\frac{dP}{dV} > 0$	Left of the MPP
$\frac{dP}{dV} < 0$	Right of the MPP

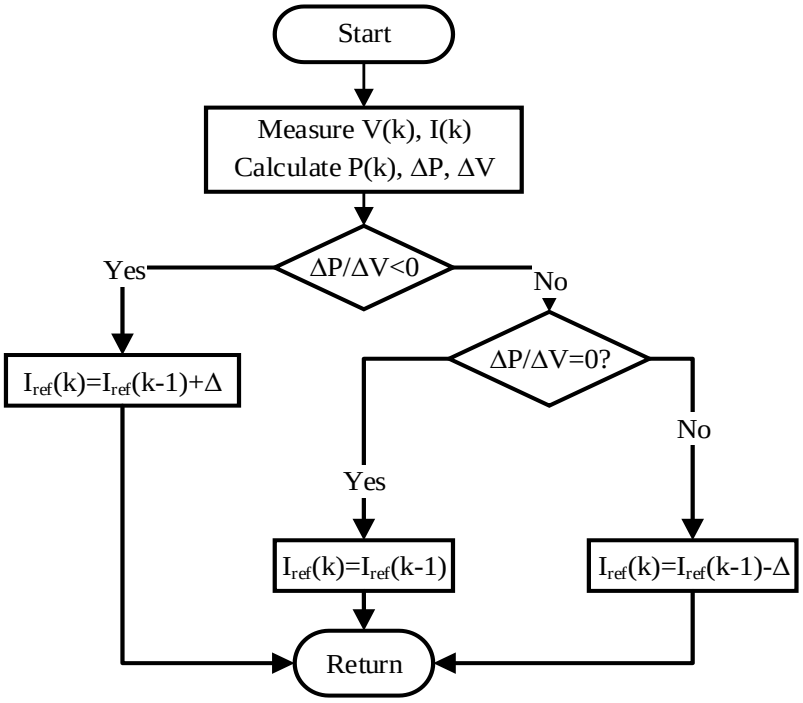

Figure 2.6. Flowchart of the IC algorithm.

2.2.2.1. Modified Incremental Conductance

A modified incremental conductance (MIC) approach has been developed, as shown in Figure 2.7. where the irradiation was adjusted to optimize the IC algorithm and minimize the oscillation that surrounded the MPP.

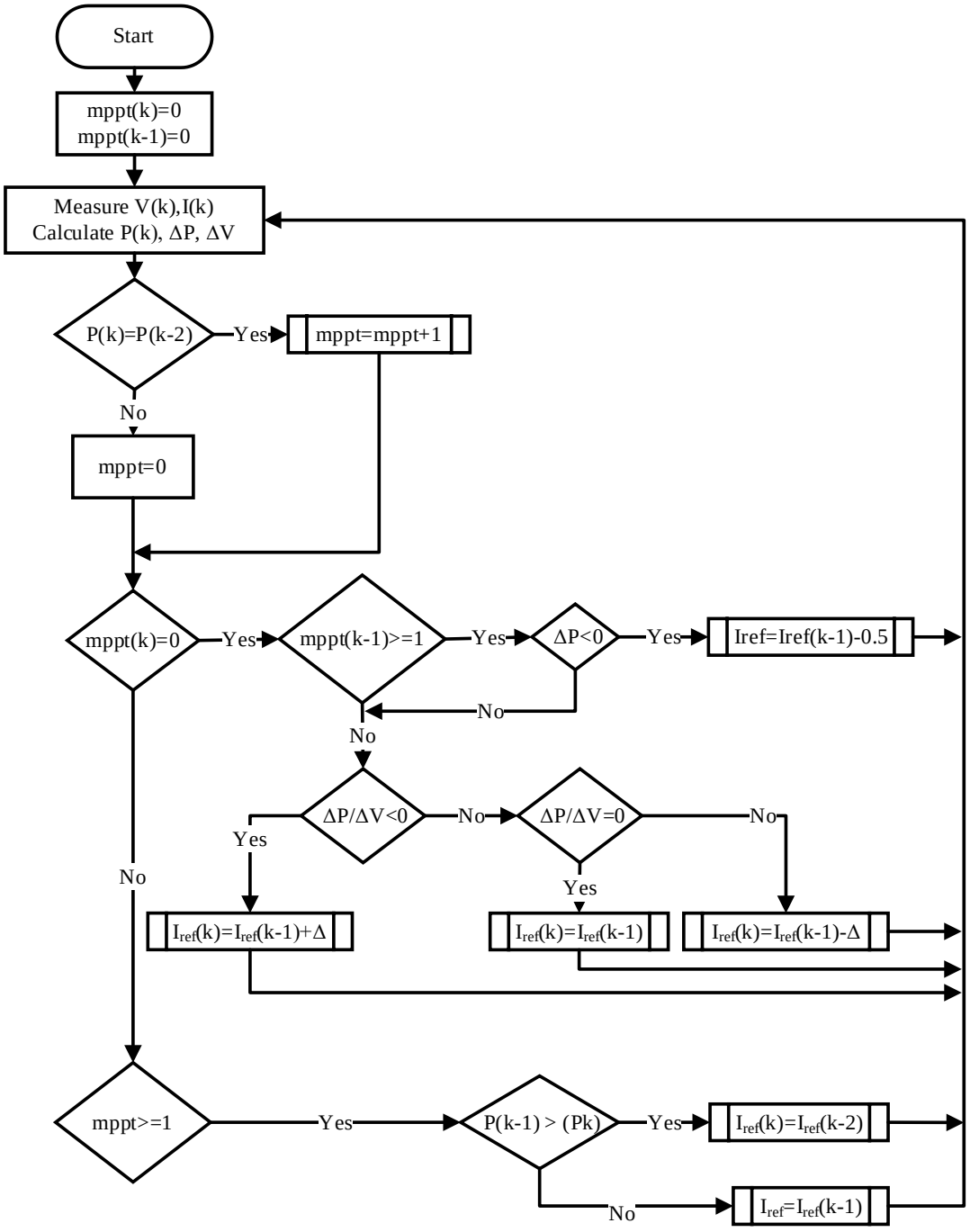

Figure 2.7. Flowchart of the MIC algorithm.

There are many MPPT techniques in the literature, and they have some advantages and/or disadvantages, as summarized in Table 2.2 [26-28].

Table 2.2. Comparison of MPPT methods [26-28].

Method	The Parameters Used	The Controlled Parameter	Advantage	Disadvantage
Open voltage	Voltage	PV voltage with constant K_{oc}	•Cheap and quick to execute. It can be carried out using a single sensor. •A simple control loop is necessary.	•The constant K_{oc} change depending on the change of temperature and radiation,
Short Circuit Current	Current	PV current with constant K_{sc}	For the use of a single sensor	•Ambient k_{sc} constant change according to the conditions, measurement of current from short circuits. •Current measurement process more costly and difficult.
Fuzzy Logic	Voltage Current	PV current with Iref	• Fuzzy Logic Systems have a simple and comprehensible structure. • You can use cheap sensors that help you keep the total complexity and cost of the device down.	•The Fuzzy logic is not always accurate, so the conclusions are reliant on assumptions. • Some fuzzy time logic is confused with probability theory and the terminology.
P&O	Voltage Current	PV current with I_{ref}	• Simple to carry out	• The MPPT at steady-state cannot catch. •Around MPPT oscillates.
IC	Voltage Current	PV current with I_{ref}	• Determines the direction of perturbation in changing weather conditions.	• Its steady-state release is less than P&O.

PART 3

DC-DC CONVERTERS

DC-DC converters receive a DC voltage from the input and deliver the different DC voltage levels to the output [13]. Between the load and the PV array, DC-DC converters are often utilized in solar power systems to get load matching and thus MPPT [14]. The used block diagram is given in Figure 3.1.

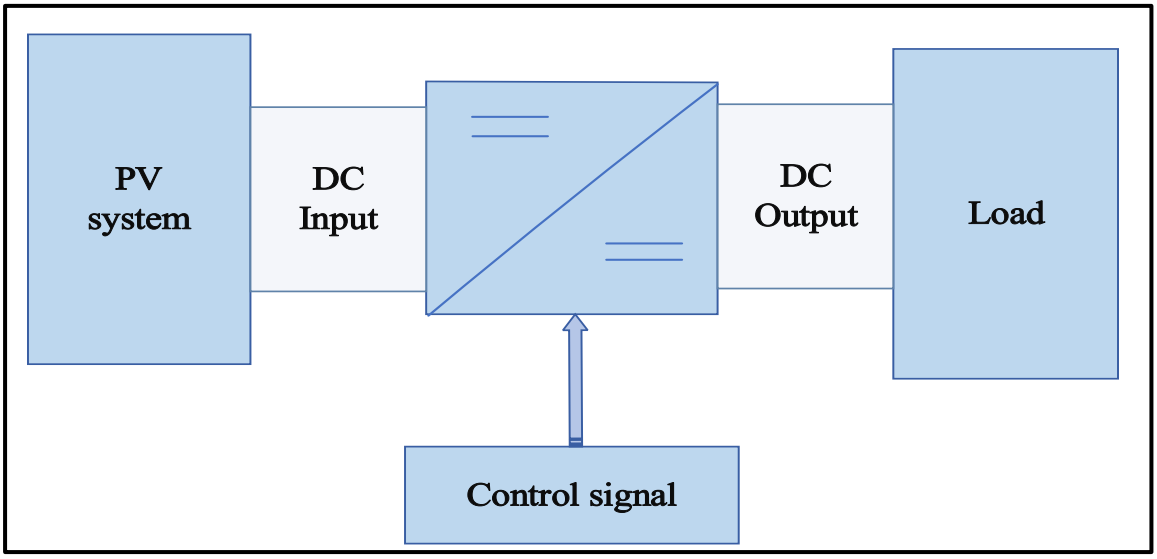

Figure 3.1. Block schematic of a general DC-DC converter.

In a wide range of applications, from low-power to high-power, the DC-DC converter is important. Any system's objective is to highlight and attain efficiency to meet the system's requirements and demands. In this field, several topologies have been devised. However, these topologies may be considered separate or a mixture of the three basic topologies, buck, boost, and flyback [19].

The purpose of the DC-DC converter is to alter the duty cycle of the converter according to the desired output voltage [20].

DC-DC converters mainly consist of two types:

1. Isolated converter type:

- Half-bridge converter
- Full bridge converter
- Flyback converter

2. Non –isolated converter type:

- Buck-boost converter
- Cuk converter
- Sepic converter
- Buck converter
- Boost converter

The DC-DC converters work by turning on and off a switching mechanism on and off at regular intervals. The Buck converter is used to get a lower voltage at the output. On the other hand, the Boost converter is used for vice versa. The Buck-Boost converter may raise or reduce the input voltage while reversing the polarity [17]. The output voltage magnitude of the Cuk converter might be lower or greater than the input voltage, and there is a polarity reversal on the output [14]. The Sepic can generate a voltage of output that is either lower or higher than the input value but without polarity reversal [14].

3.1. BUCK CONVERTER

A Buck converter is a DC-DC converter that has a lower output voltage than the input voltage. Figure 3.2. depicts the basic Buck converter circuit [20]. When the switch S1 is closed, the current i_L passes through the inductor to the load, charging the inductor L by increasing its magnetic field and voltage output. The output voltage is eventually reaching the desired value. The switch S1 will then be turned off. The current will pass via the recovery diode D. Although the current continues to flow through inductor L, it is discharged. Before the inductor is completely drained, S1 is turned on, D is turned off, and the cycle continues. The duty cycle of the switch S1 can be changed to adjust the ratio between input and output voltage.

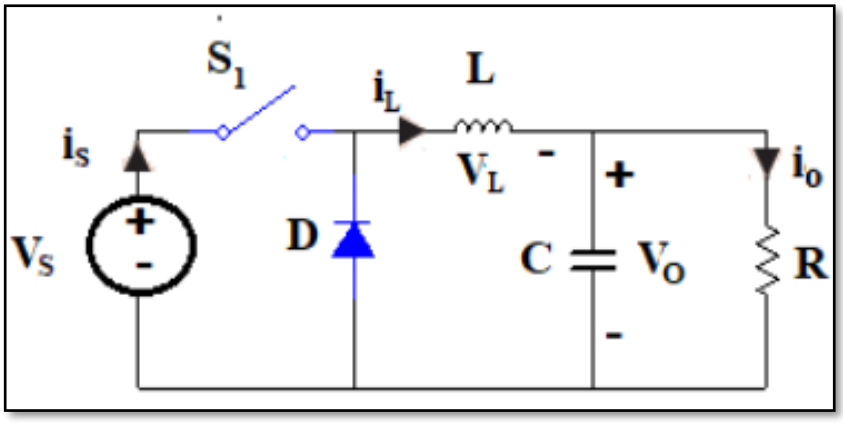

Figure 3.2. Basic buck converter circuit [20].

3.1.1. MODEL OF THE BUCK CONVERTER

The moving average in the state-space model is employed in the linearization of the Buck converter [21]. The method is frequently utilized in the modelling of PWM-controlled switching power converters. It entails calculating the circuit's weighted average state concerning the operational duty cycle throughout the switching time [22].

3.1.1.1. State Equations

The effects of resistive losses R_L in the inductor and resistance equivalent of the series capacitor R_{SE} were included to obtain a more accurate model for the Buck converter. The switch and the diode were considered ideal. The voltage supplied by the PV array is represented by a voltage source V_{pv} and the load current disturbance by I_{pv} [22]. The battery is simulated as a simple resistive load R. Figure 3.4. shows the Buck circuit used in the model [22].

In a Buck converter, the control system regulates the switching of the electronic switch according to a duty cycle d, which corresponds to the amount of time of the switching period T, wherein the switch is conducting. The equivalent Buck circuit, during the

time interval dT the switch is on, as given in Figure 3.4. When the switch is off, during the time (1-d)T, the equivalent circuit is that of Figure 3.4.

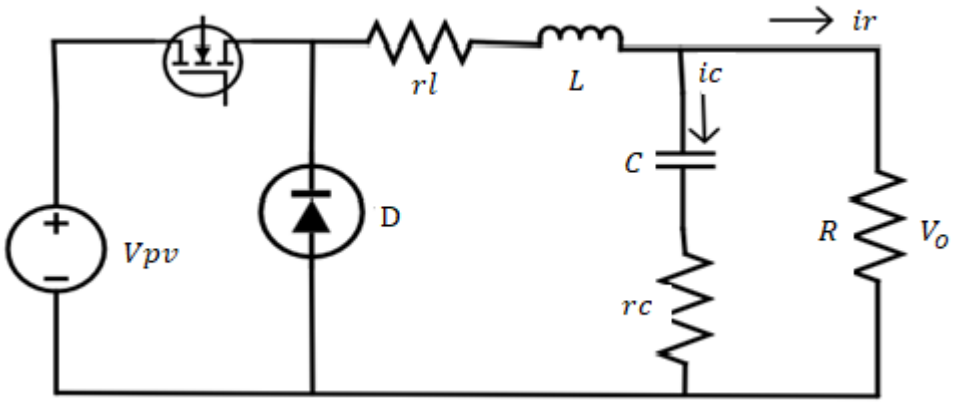

Figure 3.3. Buck converter model.

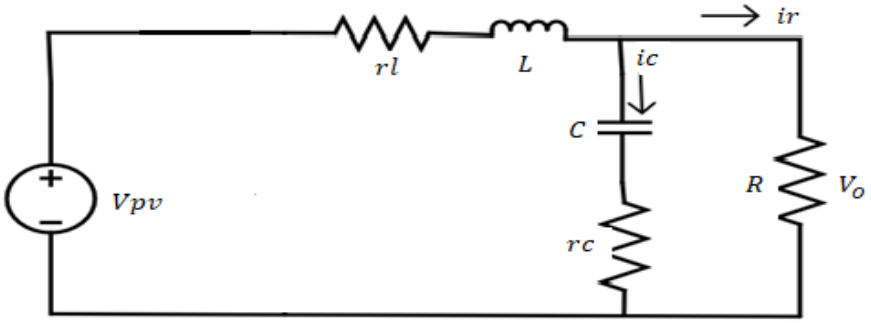

(a)

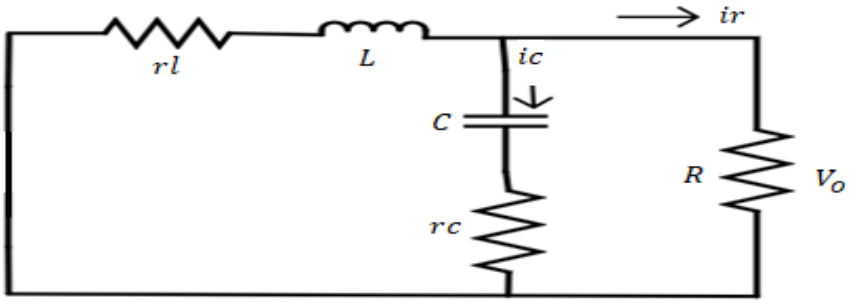

(b)

Figure 3.4. Buck circuit with the switch is (a) On, (b) Off.

To write the state equations for each subinterval:

When the switch (on), Equation 3.1 and 3.2 are obtained.

$$C\frac{dv_c}{dt} = -\frac{v_c}{R} - \ i_c \ \frac{r_c}{R} + i_{PV} \ + i_L(t) \tag{3.1}$$

$$L\frac{di_L}{d_t} = - \ i_L(t)\, r_L - \ v_c(t) - i_c r_c \ + V_{pv} \tag{3.2}$$

When the switch (of), Equation 3.3 and 3.4 can be obtained.

$$C\frac{dv_c}{dt} = -\frac{v_c}{R} - \ i_c \ \frac{r_c}{R} + i_{PV} \ + i_L(t) \tag{3.3}$$

$$L\frac{di_L}{d_t} = - \ i_L(t)\, r_L - \ v_c(t) - i_c r_c \tag{3.4}$$

3.2. DC-DC BUCK CONVERTER DESIGN

The parameters of the PV panel used in the thesis are given as shown in Table 3.1.

Table 3.1. Parameters for the 1-80 NP photovoltaic panel.

Parameters	Values
Maximum power current, Imax.	2.22A
Maximum power voltage, Vmax.	18V
Maximum power, Pmax.	39.96 W
Short circuit current, I_{sc}.	2.58A
Open circuit voltage, V_{oc}.	22.1
Short circuit temperature coefficient.	1.1e-3 (A/°C)
Numbers of cell in series.	36

As shown in Figure 3.2. the Buck converter consists of four components: a power MOSFET utilized as a switch S, a diode D, an inductor L, and a filter capacitor C. Because of their high speeds, Power MOSFETs are the most often utilized controlled switches in DC-DC converters.

Design parameter values are selected as minimum 500 W/m^2 and maximum 1000 W/m^2. Maximum and minimum voltages to MPP are selected as 3V. The following assumptions are used to begin the study of the Buck converter in Figure 3.3.

- The diode and the power MOSFET are ideal switches.
- The switching frequency is F_s=20kHz.
- Maximum and the minimum input voltage is $V_{in\text{-}max}$=18+3V, $V_{in\text{-}min}$=18-3V.
- Maximum and the minimum output voltage is $V_{o\text{-}max}$=14.4V, $V_{o\text{-}min}$=10.8V [22]
- Maximum and minimum power of a PV panel is P_{max} =39.96W, P_{min}=20.08W
- Maximum and minimum duty cycle (D) respectively found as:
- Maximum and minimum output load current which is given by;

$$I_{o-max} = \frac{P_{max}}{V_{o-min}} \tag{3.5}$$

$$I_{o-max} = \frac{39.96}{10.8} = 3.7A$$

and

$$I_{o-min} = \frac{P_{min}}{V_{o-max}} \tag{3.6}$$

$$I_{o-min} = \frac{20.08}{14.4} = 1.39A$$

- Minimum and maximum duty cycle (D) respectively found as:

$$D_{min} = \frac{Vo-min}{V_{\text{in-max}}} \tag{3.7}$$

$$D_{min} = \frac{10.8}{21} = 0.514$$

and

$$D_{max=}\frac{Vo-max}{V_{in-min}} \quad (3.8)$$

$$D_{max=}\frac{14.4}{15}=0.96$$

- Maximum and minimum load resistance respectively which is given by;

$$R_{Lmax}=\frac{V_{o-max}}{I_{o-min}} \quad (3.9)$$

$$R_{Lmax}=\frac{14.4}{1.39}=10\ ohm$$

and

$$R_{Lmin}=\frac{V_{o}\_min}{I_{o-max}} \quad (3.10)$$

$$R_{Lmin}=\frac{10.8}{3.7}=2.9ohm$$

The efficient of system design is 0.85 so the L is ;

- The inductance value of system design is given by;

$$L_{min}=\frac{R_{Lmax*}\left(\frac{1}{efficient}-D_{min}\right)}{2*f_s} \quad (3.11)$$

$$L_{min}=\frac{10*\left(\frac{1}{0.85}-0.514\right)}{2*20*10^3}=151*10^{-6}\,H$$

and

$$\Delta_{iL}=\frac{V_O*1-D_{min}}{f_s*L\_min} \quad (3.12)$$

$$\Delta_{iL}=\frac{12*(1-0.514)}{20*10^3*151*10^{-6}}=1.93\ \text{A}$$

- Maximum Equivalent Series Resistance (ESR) for C is:

$$r_{cmax} = \frac{V_r}{\Delta_{iL}} \tag{3.13}$$

and the ripple voltage for 1% is

$$V_r = \frac{V_o}{100} \tag{3.14}$$

$$V_r = \frac{12}{100} = 0.12V$$

$$r_{cmax} = \frac{0.12}{1.93} = 62 * 10^{-3}$$

- A minimum capacitance (C) of system design which is given by

$$C_{\min\,(on)} = \frac{D_{max}}{2 * f_s * r_{cmax}}$$

$$C_{\min\,(on)} = \frac{0.96}{2 * 20 * 10^3 * 62 * 10^{-3}} = 387 * 10^{-6}\ F$$

and

$$C_{\min\,(off)} = \frac{1 - D_{min}}{2 * f_s * r_{cmax}} \tag{3.15}$$

$$C_{\min\,(off)} = \frac{1 - 0.514}{2 * 20 * 10^3 * 62 * 10^{-3}} = 192 * 10^{-6}\ F$$

- the Bulk input conductance value of system design which is given by,

$$C_{bulk} = \frac{P_{max}}{2 * \pi * f_s * V_{max} * V_r} \tag{3.16}$$

$$C_{bulk} = \frac{39.96}{2 * \pi * 20 * 10^3 * 18 * 0.12} = 147 * 10^{-6}\ F$$

For this studies the C_{bulk} value is selected as $50* 10^{-6} F$ because it has good response for the control signal.

PART 4

BATTERY MANAGEMENT SYSTEM

Nearly every portable gadget has a battery, and practically everyone charges their batteries daily. Batteries are chemical energy storage devices that store electrical energy, subsequently used to power a device or circuit. Any system that monitors and manages batteries is referred to as a battery management system (BMS). Because batteries are used in almost all portable equipment that requires electricity, battery management solutions are in high demand [27].

LA batteries, lithium-ion batteries, nickel-cadmium batteries, and nickel-metal-hydride batteries are all examples of rechargeable batteries. Because it is both efficient and cheap, the Lead-acid battery is one of the most often used rechargeable batteries. Other significant features of a LA battery include are its tolerance to overcharging, ability to produce high current, and low impedance [28]. Batteries are mostly used for solar energy storage. Because of its autonomy and high Depth of Discharge (DOD), which may approach 80% in these sorts of batteries, valve valve-controlled LA batteries are extensively utilized in solar applications [29].

4.1. LEAD-ACID BATTERY

Gaston Planté, a French scientist, created the Lead-Acid (LA) battery in 1859, which is essentially a number of lead and lead oxide plates submerged in sulfuric acid electrolyte with separators in between. There are two general LA battery types: Both are constructed roughly the same way, with minor variations in different characteristics and applications [27]. The nominal cell voltage of LA cells is 2.0 volts per cell, with 12 volts per cell. A LA battery is made up of six cells linked in series. The charge voltage value varies between 2.30V and 2.45V per cell. Sulfation occurs on the plate, which is negative when the voltage threshold is set to a too low value. In contrast, grid corrosion occurs on the plate, which is positive when the voltage threshold is too high,

resulting in gassing see Table 4.1. The benefits and drawbacks of charging the low and high voltage thresholds are listed below [28].

Table 4.1. Battery University provides information on the effects of charge voltage on a LA battery [27].

	2.30V to 2.35volts /cell	**2.40V to 2.45 volts /cell**
Advantages	Charge temperatures can surpass 30°C (86°F) throughout the battery's maximum service life.	Capacity values that are higher and more consistent Sulfation are reduced.
Disadvantage	The time for change is slow. Readings on capacity may be unreliable and decreasing with each cycle. Sulfation can occur without the presence of an equalizing charge.	Corrosive and gassing potential It requires continuous water and is not suited for charging at high room temperatures, resulting in severe overchange.

New markets for energy storage in rechargeable batteries are driven by development in renewable energy, the demand for lower transportation emissions, and the rapid advancement of communications technology, in addition to basic economic growth for existing uses. Lead-acid batteries are still the most affordable and frequently used option. Still, technology is fast shifting toward lithium-ion and other new solutions, such as post-lithium technologies and eventually fuel cell batteries. Overall battery markets are expected to expand at a rate of 7.7% per year through 2020, with Lead-acid sales growing at a slower rate of 2-4 percent per year until 2025 [30].

Batteries such as Lead-acid, Lithium-ion, Nickel-Cadmium, and Nickel-Metal Hydride, are the most widely used generic and dynamic model, as represented it is blocked in MATLAB/Simulink program as given in Figure 4.1. The model parameters are generated from discharge characteristics and are assumed to be the same while recharging batteries [28]**.**

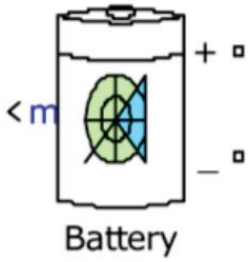

Figure 4.1. Battery block under MATLAB /Simulink.

Many researchers have given the LA battery mathematical model [27] [28] [31]. The power supply battery is frequently considered as an actual or ideal voltage source as in systems. More detailed information about the mathematical model is out of scope for this thesis.

4.2. LEAD ACID BATTERY CHARGING IMPORTANCE

Because the charging control method does not rely on precise battery current measurements, the influence of current sensor sensitivity on the battery's ultimate state of charge (SOC) is reduced. The charging control method does not rely on accurate battery current measurements, decreasing the influence of the current sensor sensitivity on the battery final state of charge. The battery lifespan is enhanced due to the higher-level state of charge operation [28].

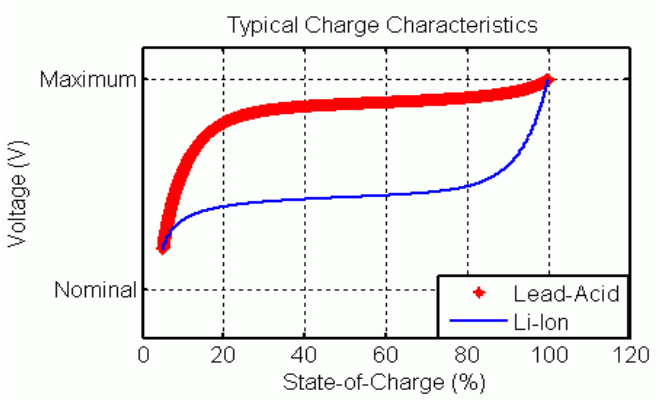

Figure 4.2. LA and Li-ion batteries charging regulation rates depending on SOC% capacity.

The charging current must be less than or equal to the maximum current of a battery.

PV power generation determines the battery-charging current, which varies depending on atmospheric conditions, whereas the level of voltage of the LA battery is determined by both the state of charge and the charging current. An MPPT method is often used for low PV output power. In other cases, the battery charging current is regulated to the maximum permitted current by increasing the quantity of energy delivered to the battery [28].

PART 5

SIMULATIONS

The MPPT algorithm applied to track MPP and PID controller used to force the system to get MPP for a standalone PV system with a DC-DC Buck converter. This thesis was designed in Matlab\Simulink as the system model shown in Figure 5.1. The model by adjusting different irradiation as (600-800-1000) W/m^2 farther and a constant temperature of 25°C, shown in Figure 5.2.

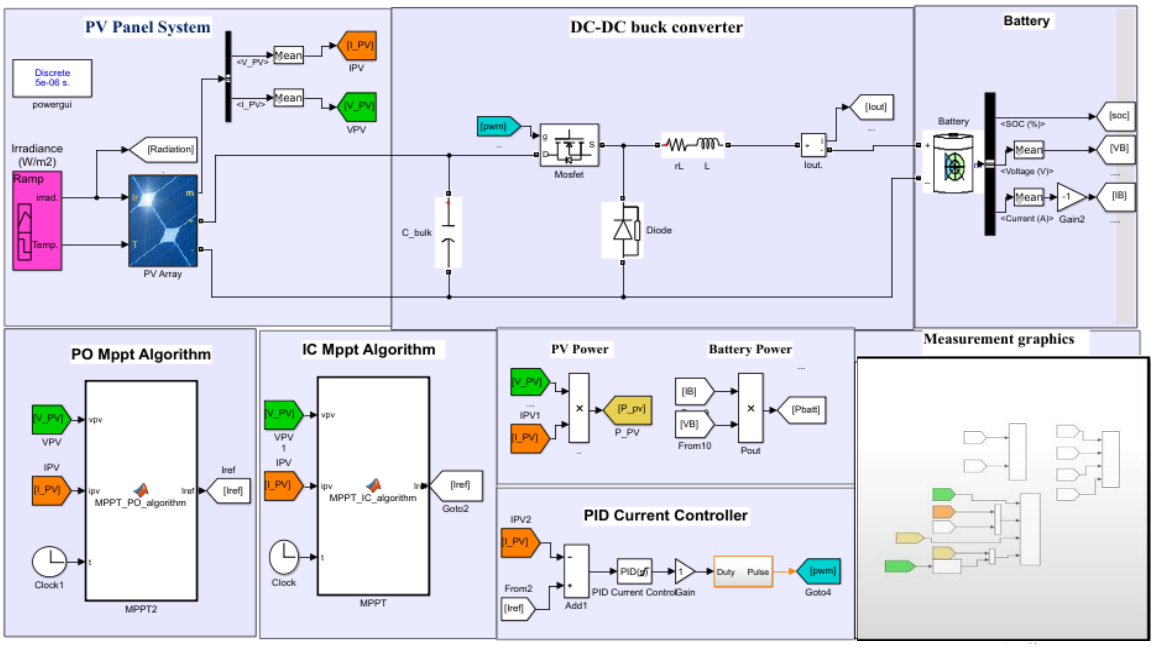

Figure 5.1. Design of Controlling the charge of the batteries in a standalone PV system.

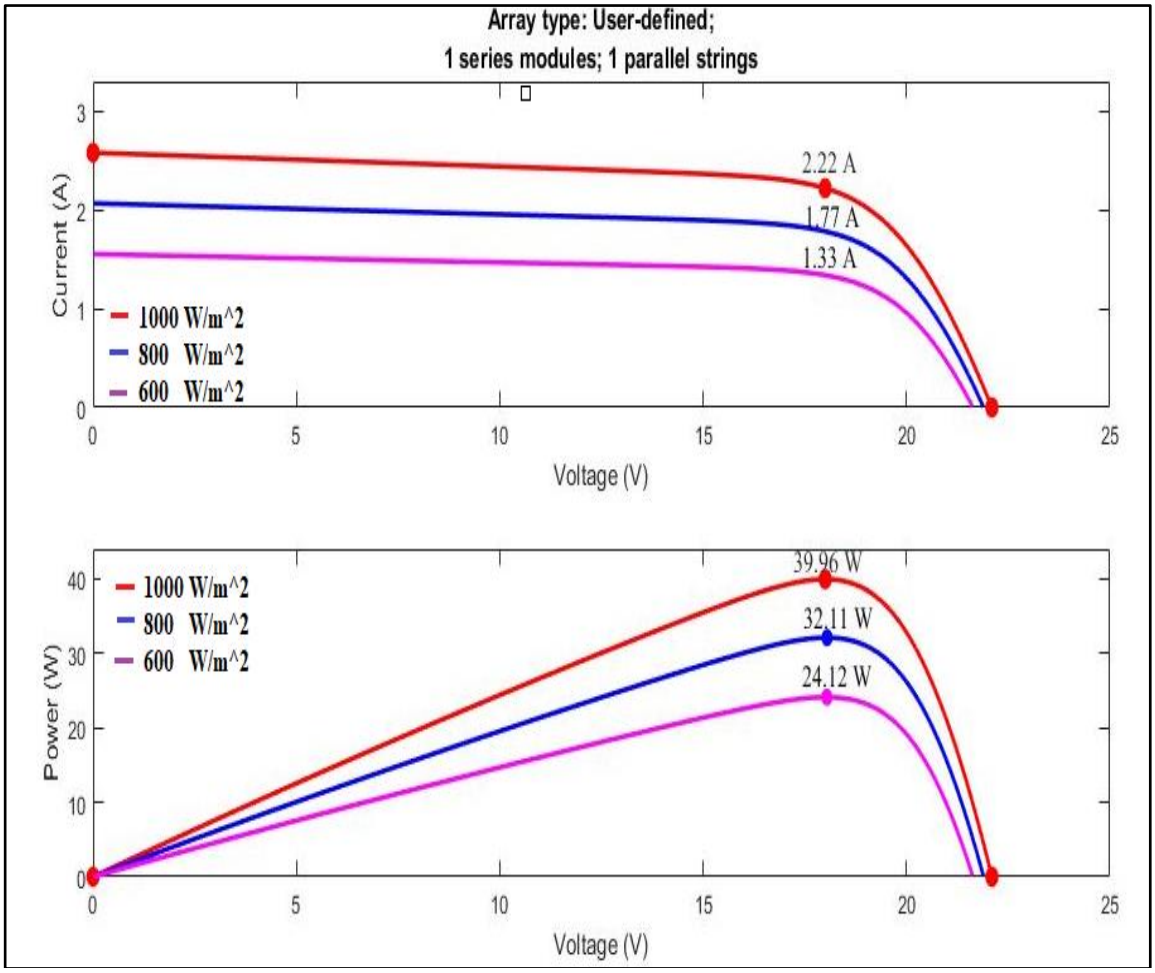

Figure 5.2. I-V and P-V characteristics of specified irradiance in (W/m^2) and constant temperature (25°C) for PV array.

As shown in Figure 5.3. at a specific time, different values of radiation to orient to the PV panel, starting from $600W/m^2$ rad. Increasing to the $1000W/m^2$ radiation, then changing by decreasing to $600W/m^2$ irradiation.

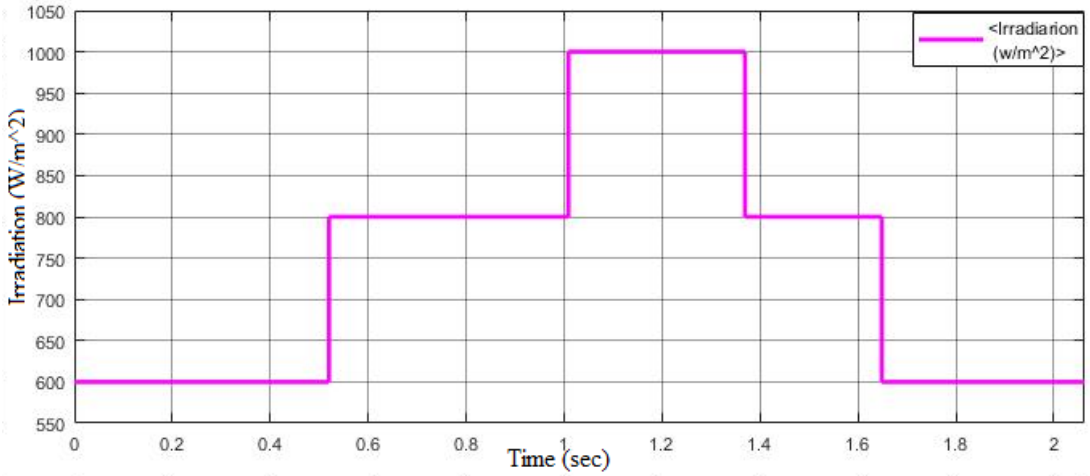

Figure 5.3. Different radiation values at a specific time.

In this research, the P&O and IC approach are utilized to compare the MPPT performance. However, choosing the ideal step size in P&O and IC in terms of the time it takes to get to the MPP and oscillation around MPP is a challenging task [32]. Smaller step sizes have drawbacks, including slower convergence to MPP and higher transient power losses. On the other hand, the bigger step sizes provide a faster convergence but suffer from oscillations around the MPP which decreases the overall efficiency of the system. To determine the best step size, the MPPT of a PV panel is acquired at various step sizes, as shown in Table 5.1.

Table 5.1 Contrasts the step sizes at different irradiation.

Step size	**Irradiation (W/ m^2)**								
	600	800	1000	600	800	1000	600	800	1000
	P_{ext} (W)			**Convergence (sec)**			**Iteration no.**		
0.01	23.73	31.52	39.19	1.45	4.55	7.85	28	42	41
0.03	24.04	32.10	39.95	0.70	2.40	4.05	14	16	16
0.05	24.09	32.06	39.89	0.60	2.05	3.70	12	10	10
0.06	24.04	32.10	39.89	0.40	2.20	3.60	8	10	10
0.07	23.95	32.09	39.62	0.70	1.90	3.30	14	12	8

As shown in Figure 5.4. the MPP at step size is 0.01, and when the step size is 0.03, the MPP is shown in Figure 5.5.

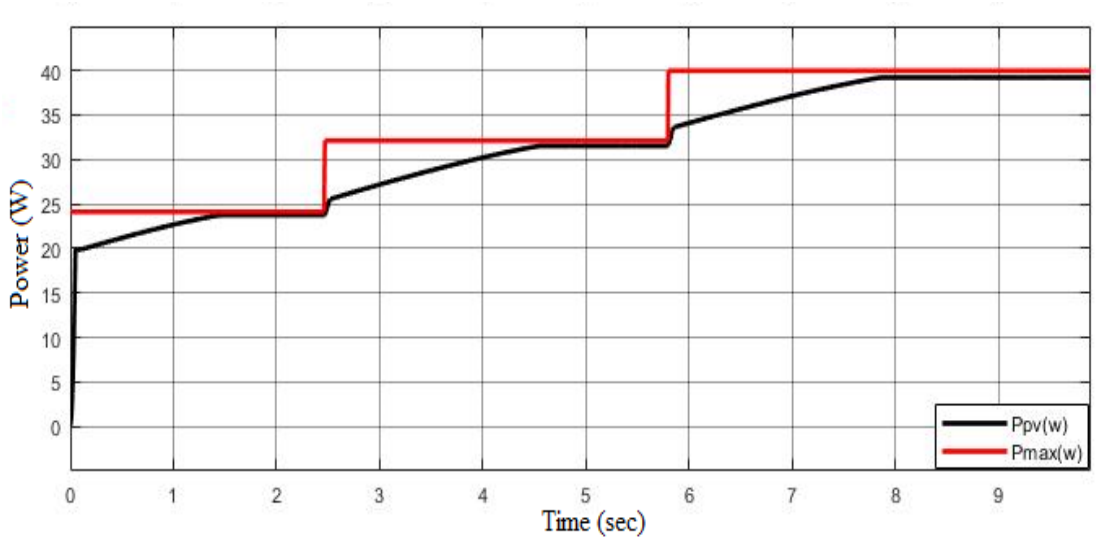

Figure 5.4. MPPT obtained by PV at step size value is 0.01.

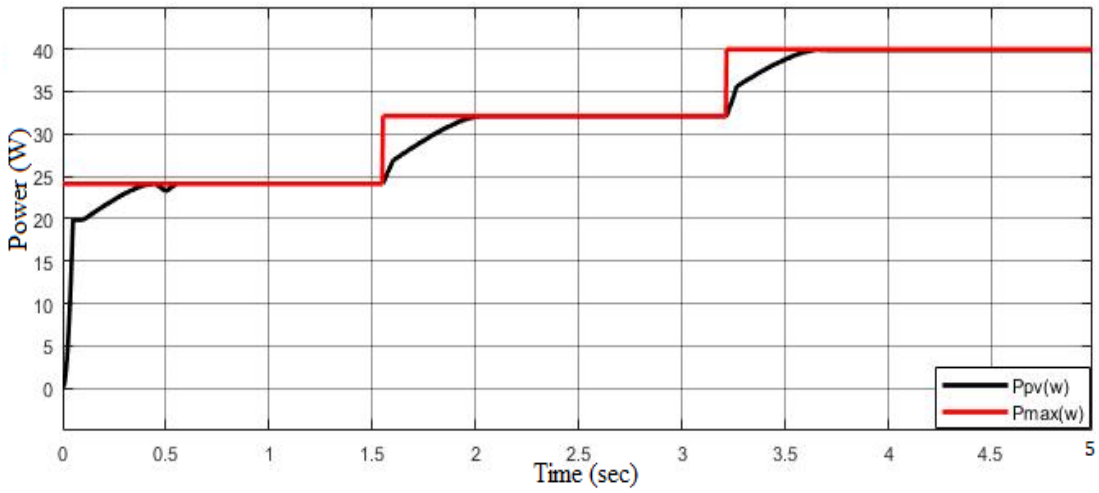

Figure 5.5. MPPT obtained by PV panel at step size value is 0.03.

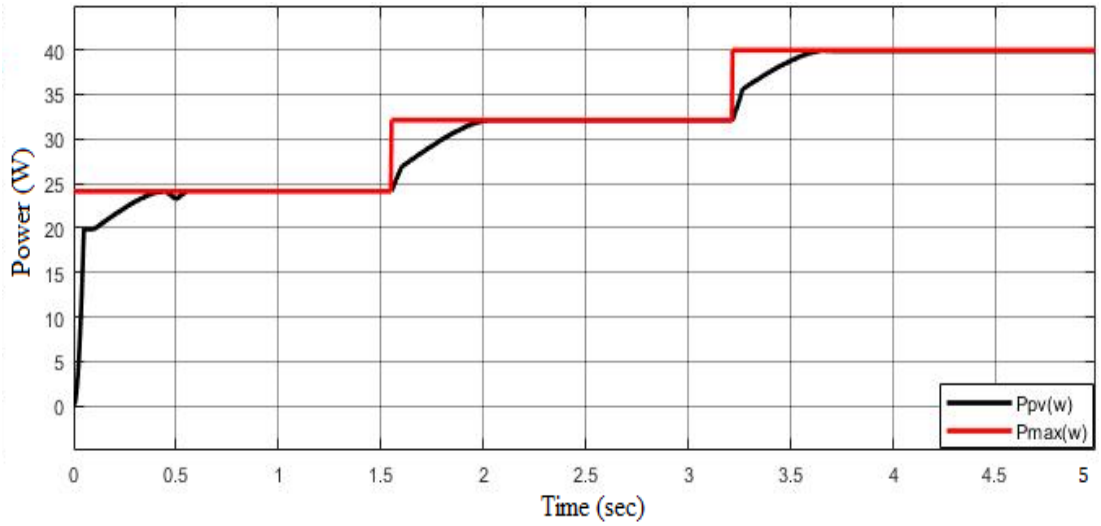

Figure 5.6. MPPT obtained by PV panel at step size value is 0.05.

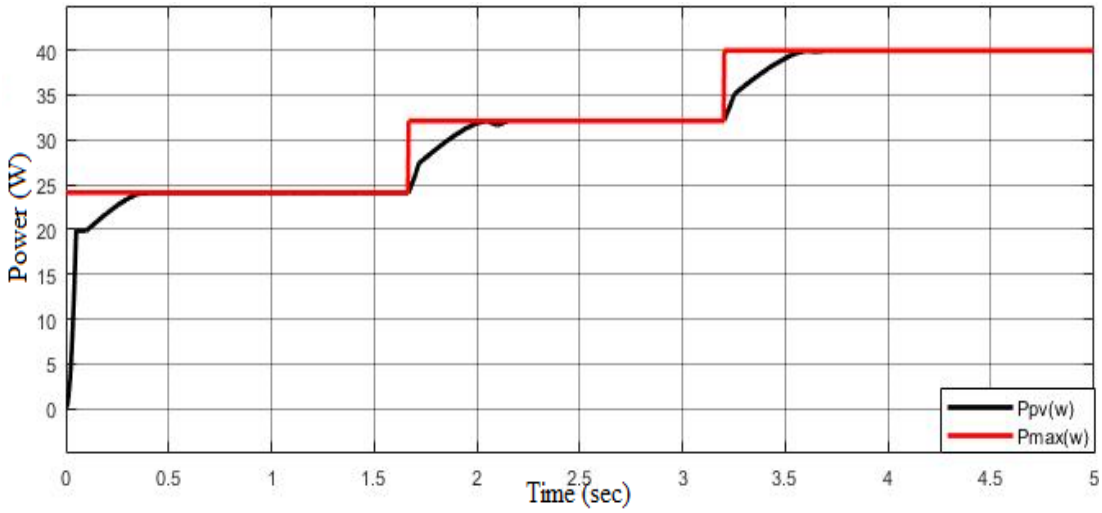

Figure 5.7. MPPT obtained by PV panel at step size value is 0.06.

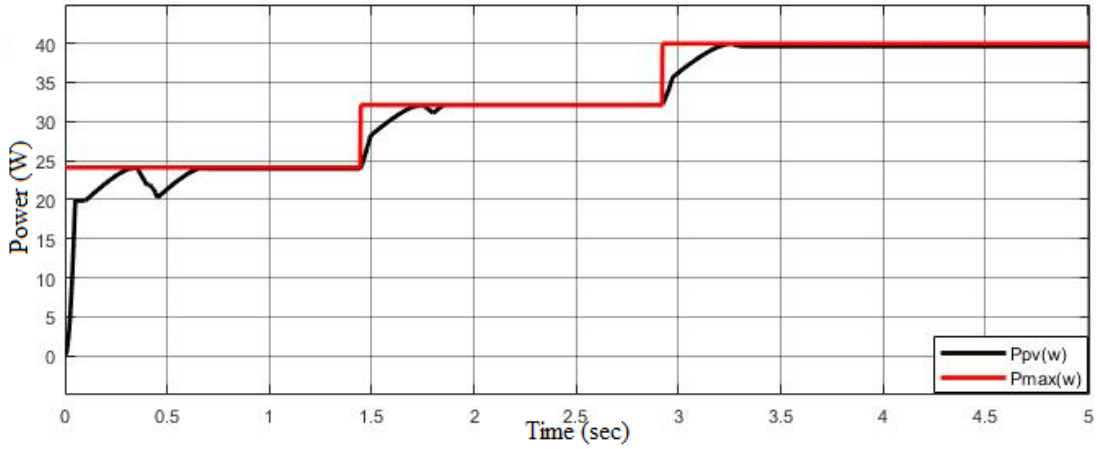

Figure 5.8. MPPT obtained by PV panel at step size value is 0.07.

Table 5.2. Contrasts the step sizes at different irradiation.

Step size	**Irradiation (W/ m^2)**								
	600	800	1000	600	800	1000	600	800	1000
	P_{ext} (W)			**P_{max} (W)**			**Steady-state error**		
0.01	23.73	31.52	39.19	24.12	32.11	39.96	0.39	0.59	0.77
0.03	24.04	32.10	39.95				0.08	0.01	0.01
0.05	24.09	32.06	39.89				0.03	0.05	0.07
0.06	24.04	32.10	39.89				0.08	0.01	0.07
0.07	23.95	32.09	39.62				0.17	0.02	0.34

As shown in Figure 5.8, the control law may be wrong for 600 W/ m^2 radiation if the step-size is increased more. Make a fair comparison between P&O and IC methods, the 0.05 step size as shown in Figure 5.6. is chosen as the optimal step size.

The other important issue is the selection of the sample time for MPPT algorithms. For this purpose, some simulation studies have been made and given as in Figure 5.9.-Figure 5.15. A time needed for MPPT in terms of these sample times is tabulated and given as in Table 5.3.

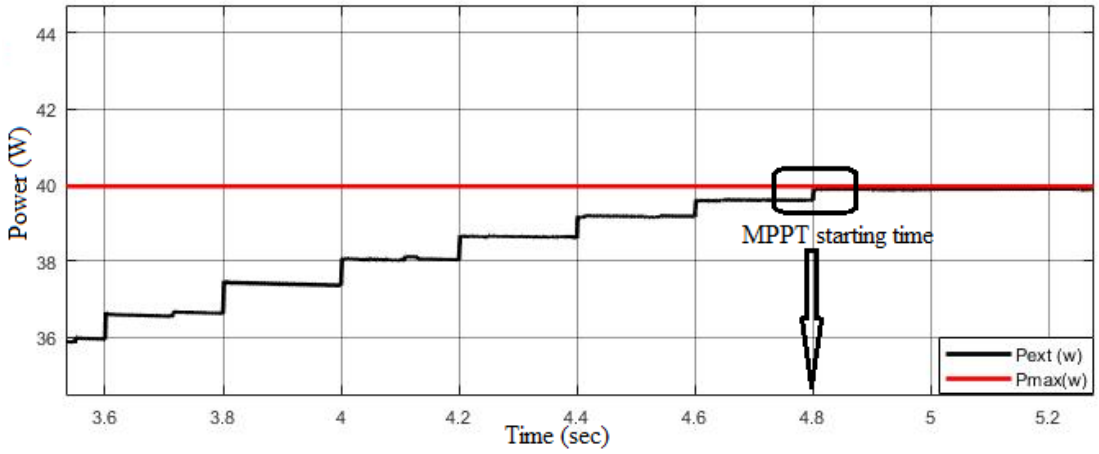

Figure 5.9. MPPT obtained by PV at sample time is 0.2 sec.

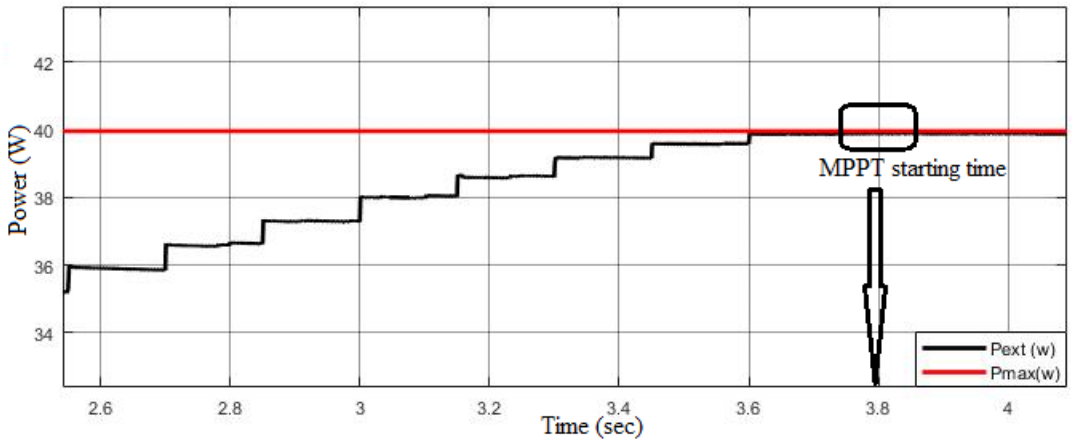

Figure 5.10. MPPT obtained by PV at sample time value 0.15 sec.

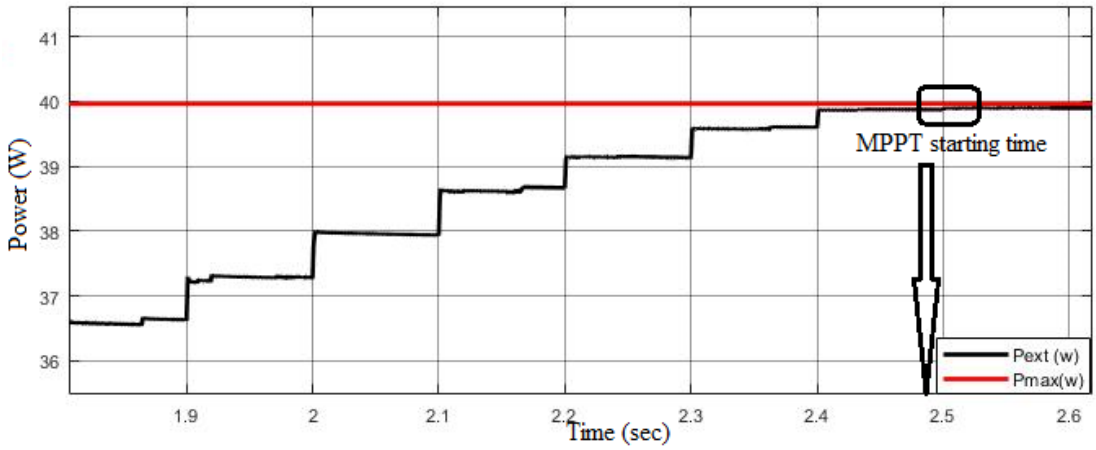

Figure 5.11. MPPT obtained by PV at sample time value 0.1 sec.

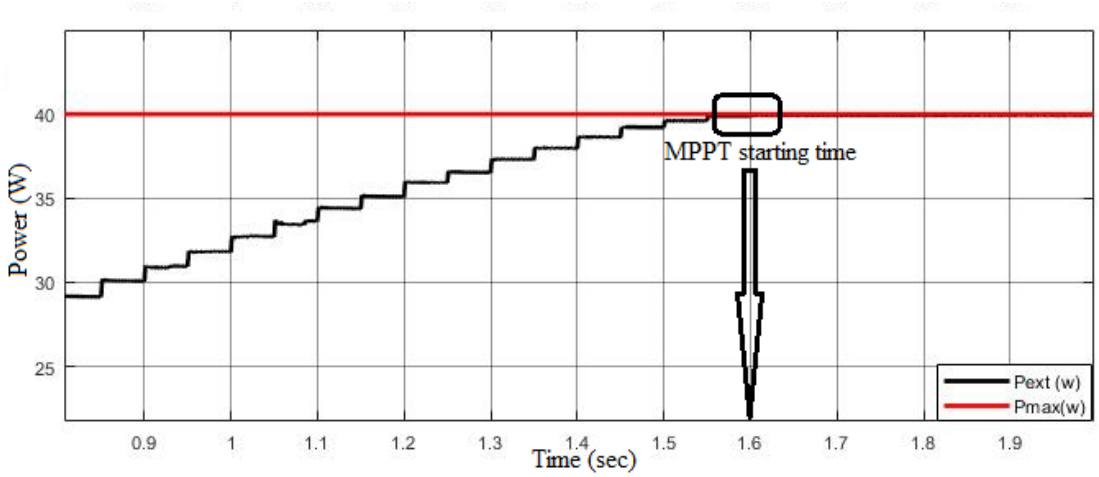

Figure 5.12. MPPT obtained by PV at sample time value 0.05 sec.

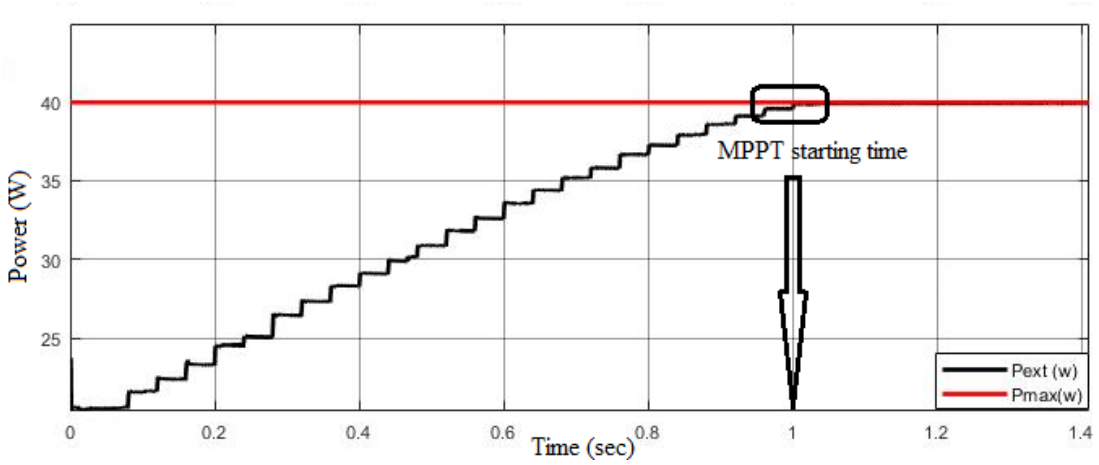

Figure 5.13. MPPT obtained by PV at sample time value 0.04 sec**.**

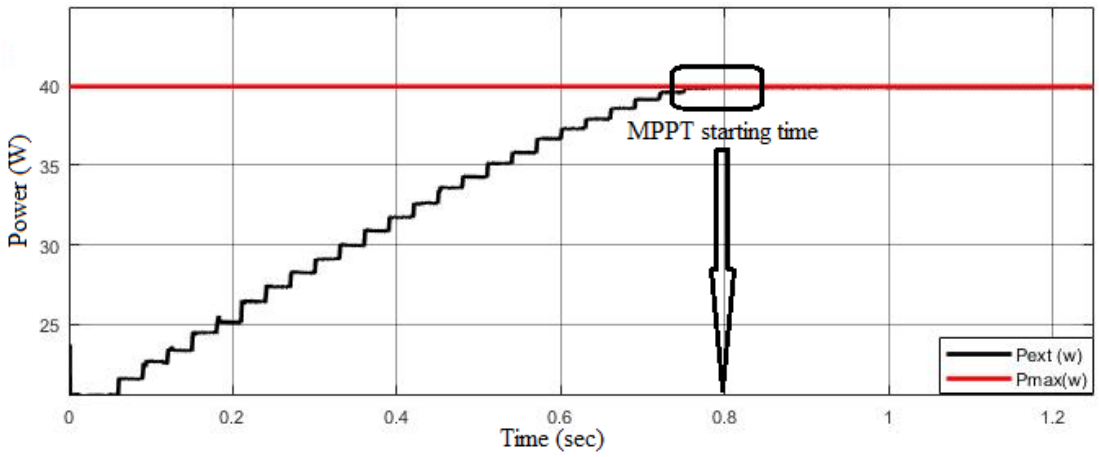

Figure 5.14. MPPT obtained by PV at sample time value 0.03 sec.

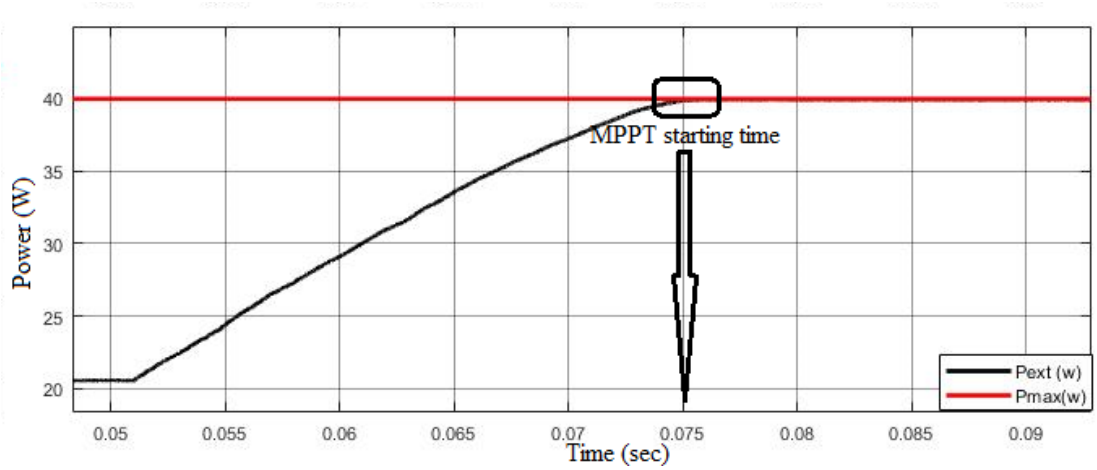

Figure 5.15. MPPT obtained by PV at sample time value 0.001 sec**.**

Table 5.3. Contrasts the sampling times of the MPPT block in MATLAB/Simulink.

Sample time (sec)	**Convergence speed of MPPT (sec)**
0.2	4.8
0.15	3.8
0.1	2.5
0.05	1.6
0.04	1.0
0.03	0.8
0.001	0.075

The time constant of the system is calculated as 30 ms. Accordingly, the sample time is tested according to the values given in Table 5.3. and it is decided to use 0.001 as the ideal sample time. The MPPT performance may not be suitable for lower sample time.

5.1. THE PERTURB AND OBSERVE (P&O) ALGORITHM

The PV current is regulated according to the reference current obtained from the MPPT

algorithm by the PID controller, as seen in Figure 5.16.

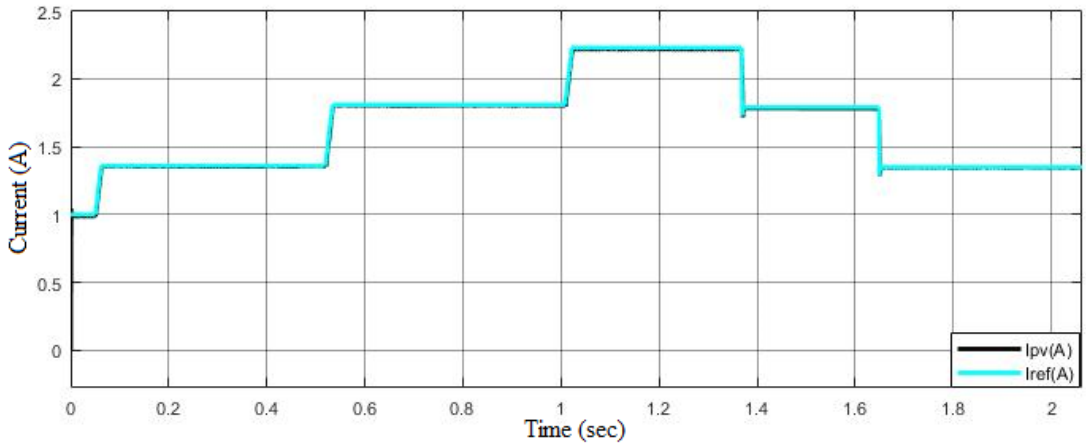

Figure 5.16. PV current with reference current for the P&O algorithm.

The PV voltage and PV power are given for the P&O algorithm, as shown below in Figures 5.17. and Figure 5.18.

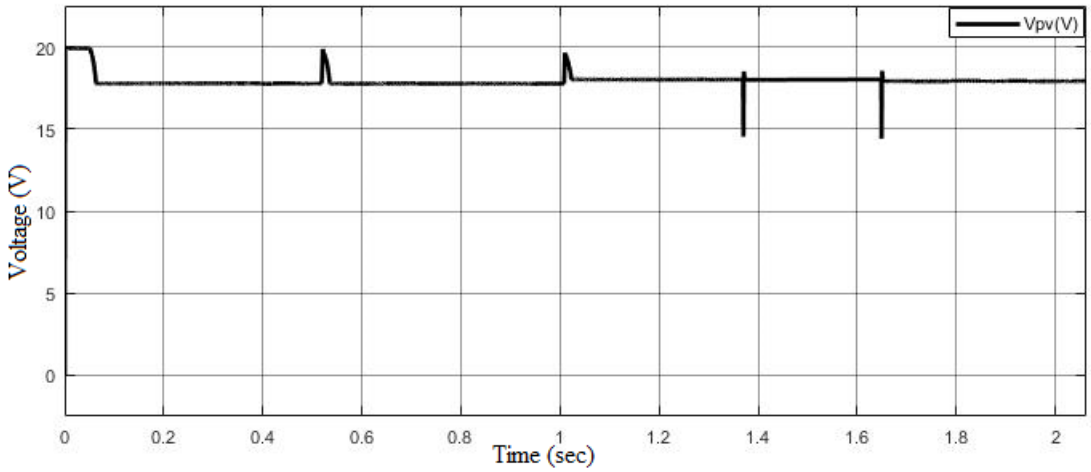

Figure 5.17. PV voltage for the P&O algorithm.

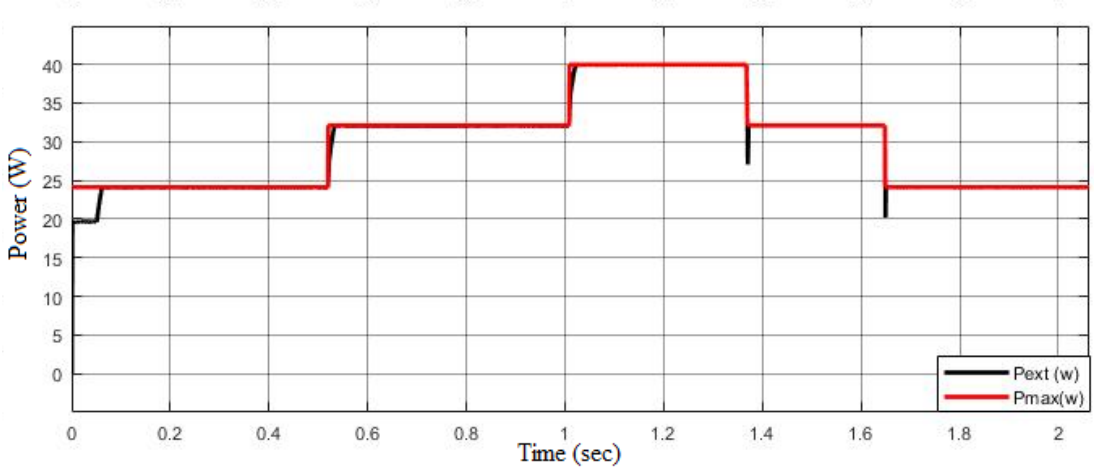

Figure 5.18. PV power for the P&O algorithm.

The LA battery's SOC, the charge current, battery voltage, and battery power, respectively, are given for the P&O algorithm, as shown in Figure 5.19-Figure 5.22.

State of Charge (SOC %)

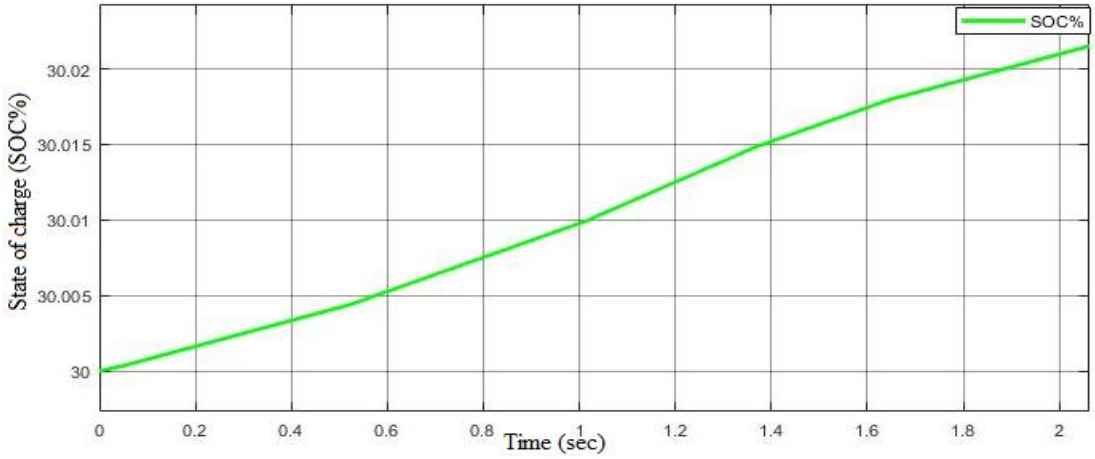

Figure 5.19. Lead-acid battery state of charge rating graphic.

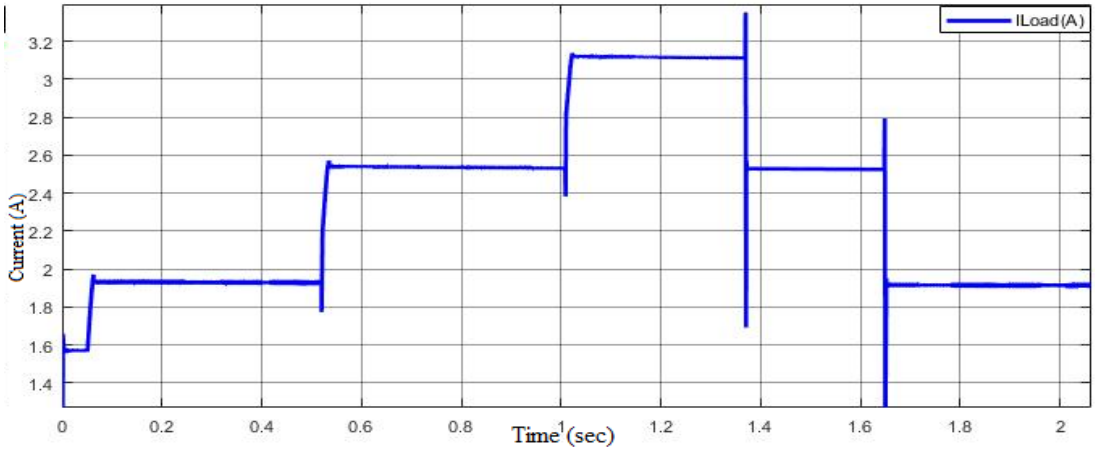

Figure 5.20. Load current for the P&O algorithm.

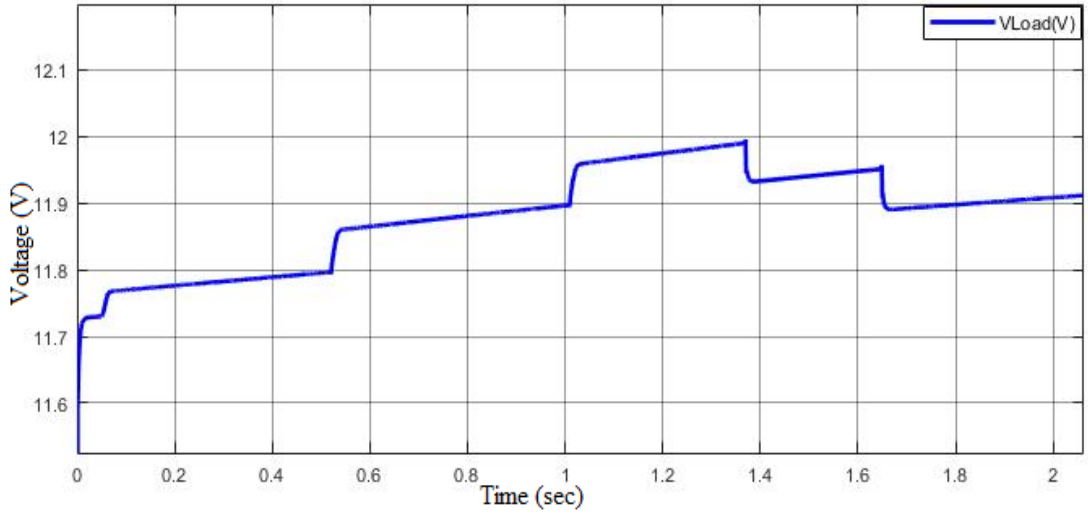

Figure 5.21. Load voltage for the P&O algorithm.

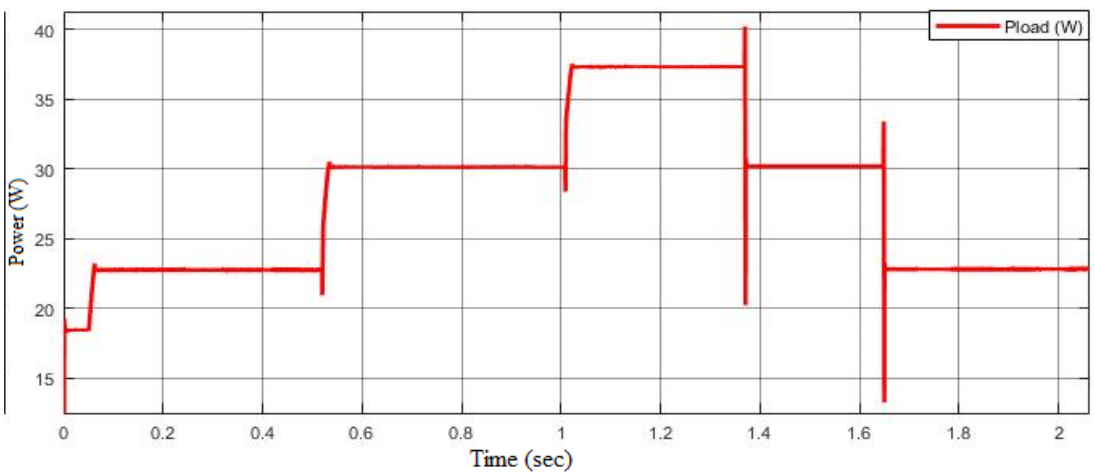

Figure 5.22. Load power for the P&O algorithm.

Charge strategies will develop in dependence on the SOC to enable complete and safe LA battery charging, as shown in Table 5.4 with taking the SOC at 30% capacity, the battery voltage is between 11V-12V, which is less than 80%-90% of the SOC, which is about 13V at maximum voltage charge. This indicated that as the SOC percentage climbed, the battery voltage charge rose.

Table 5.4. The load power, load voltage, and PV power are measured at different (SOC%) levels for P&O technique.

State of charge	**Irradiation (W/m^2)**								
	600	800	1000	600	800	1000	600	800	1000
	P_{ext}(W)			**P_{load}(W)**			**V_{load}(V)**		
30	24.07	32.09	39.24	22.72	30.06	36.72	11.75	11.86	11.95
50	24.08	32.07	39.14	22.09	30.25	36.76	12.17	12.26	12.36
80	24.06	32.08	39.19	22.91	30.42	37.06	12.59	12.75	12.92
90	24.07	32.08	39.18	23.11	30.61	37.19	12.81	13.02	13.21

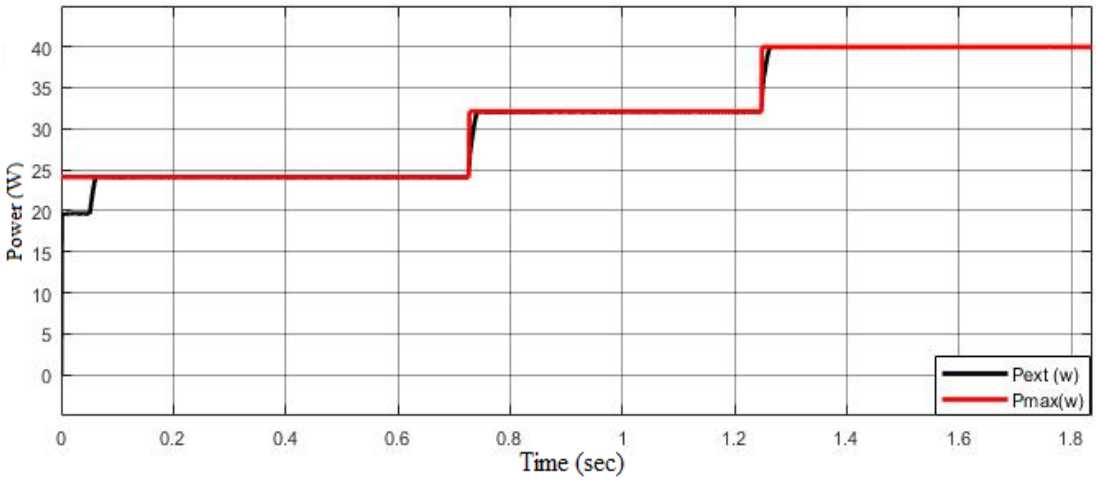

(a)

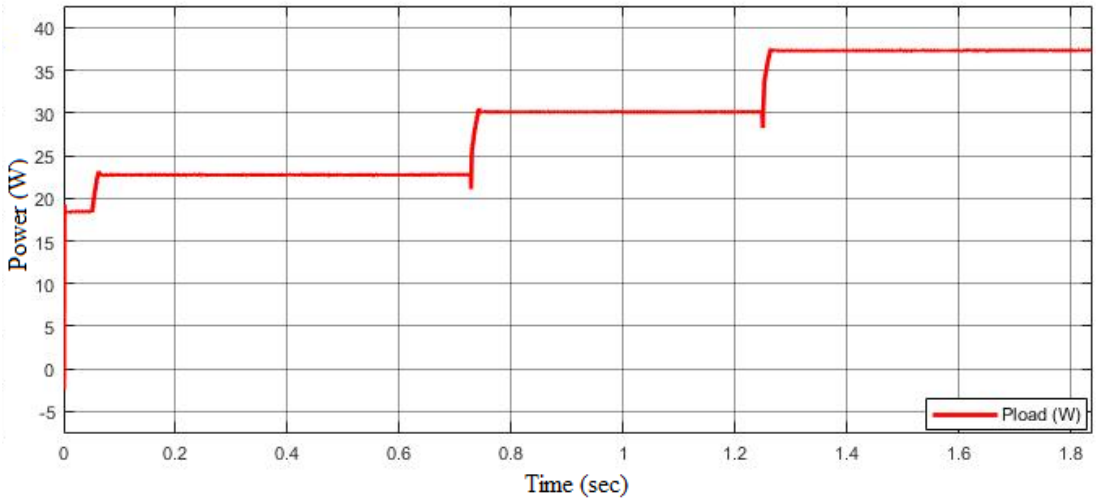

(b)

Figure 5.23. (30%) battery charge capacity graphic of (a) PV power, (b) Battery power.

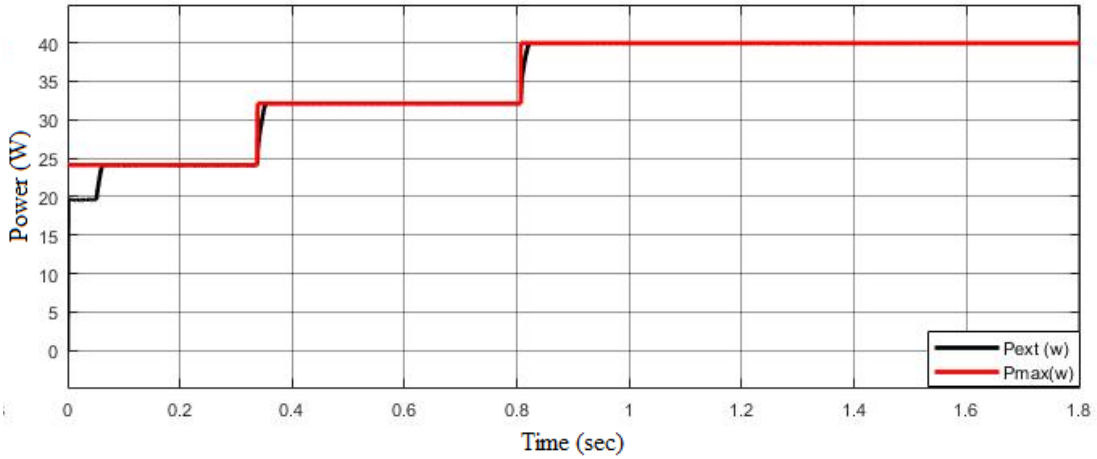

(a)

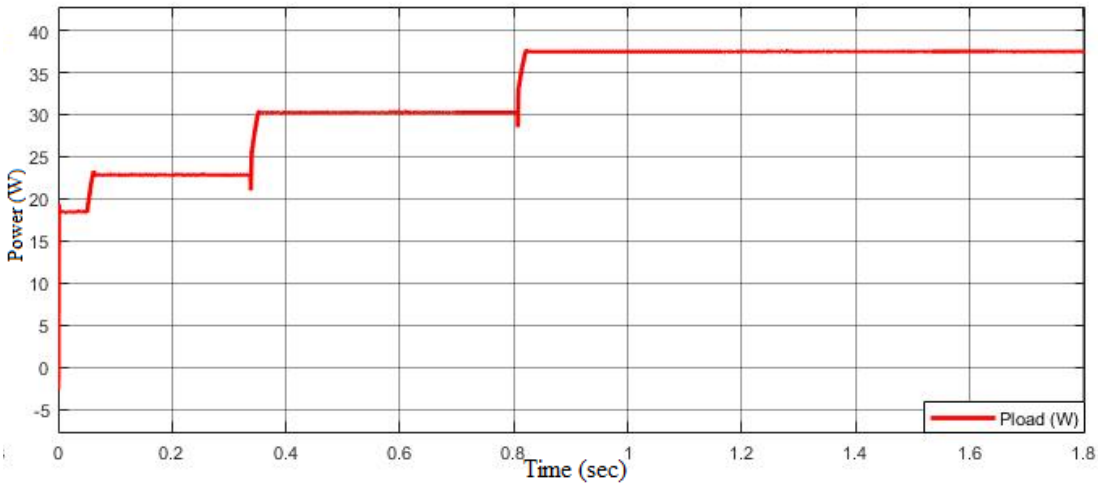

(b)

Figure 5.24. (50%) battery charge capacity graphic of (a) PV power and (b) Battery power.

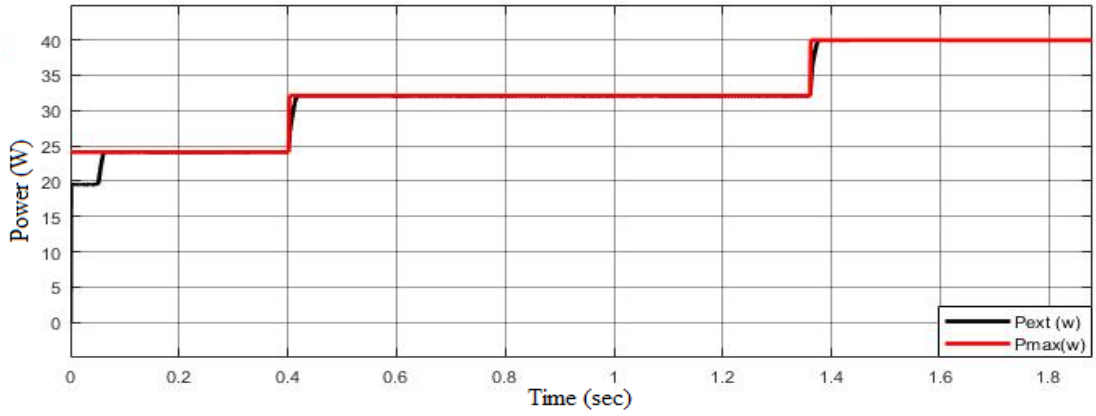

(a)

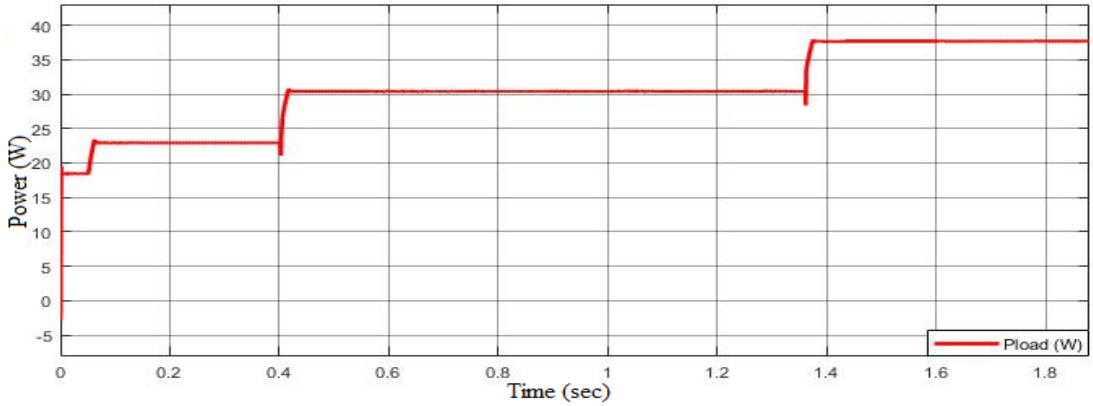

(b)

Figure 5.25. (80%) battery charge capacity graphic of (a) PV power and (b) Battery power.

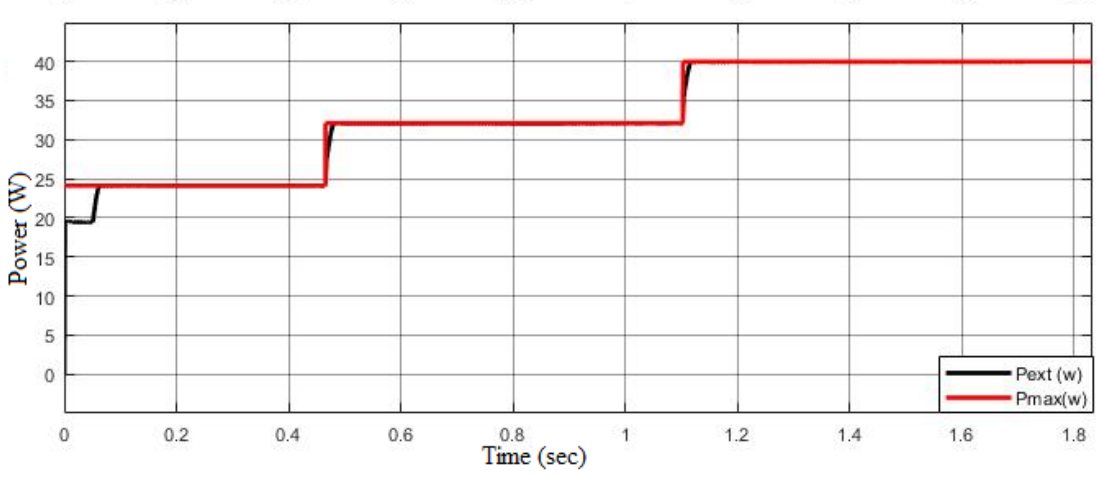

(a)

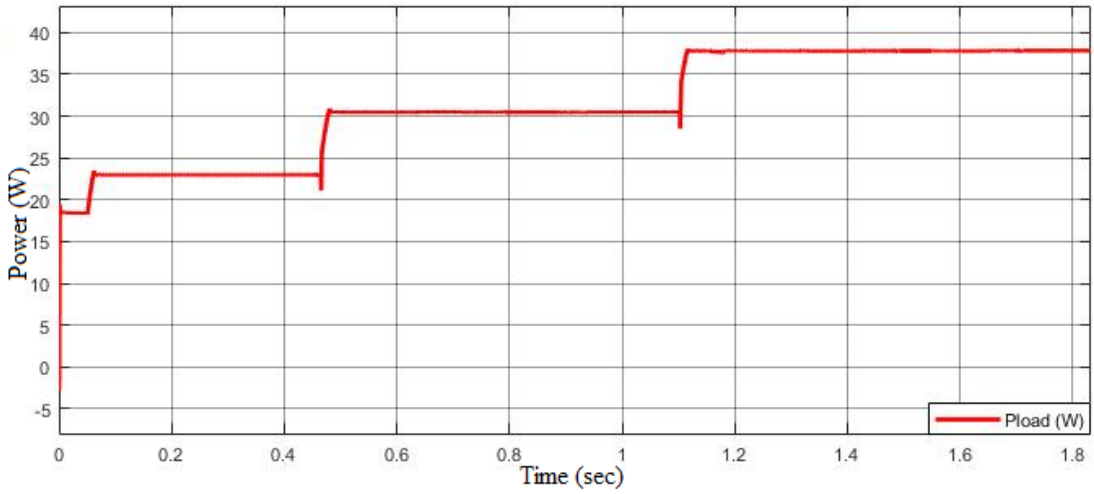

(b)

Figure 5.26. (90%) battery charge capacity graphic of (a) PV power and (b) Battery power.

5.2. THE INCREMENTAL CONDUCTANCE (IC) ALGORITHM

The IC algorithm tracks the MPP to control the battery charging current at 30% SOC, as shown in Figure 5.27. The algorithm started with 600 W/m^2 radiation and oriented the power to the maximum point. Therefore it had to improve the irradiation for the PV system to 800 W/m^2 and subsequently to 1000 W/m^2 until it reached the MPP.

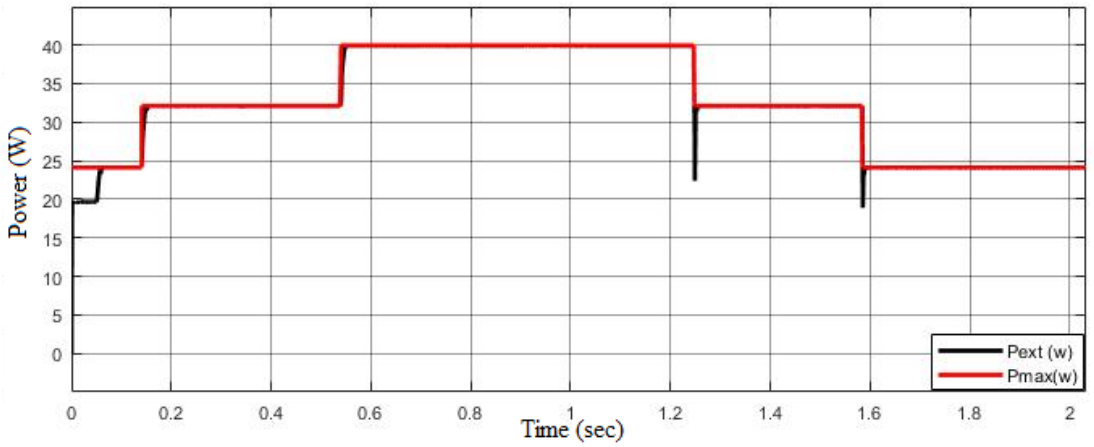

Figure 5.27. PV power for the IC algorithm.

The PV voltage and PV current are supplied for the IC algorithm as shown in Figure

5.28, Figure 5.29. Then the battery charge current, battery voltage, and battery power are given for the IC algorithm as shown in Figures 5.30, Figure 5.31, and Figure 5.32, respectively.

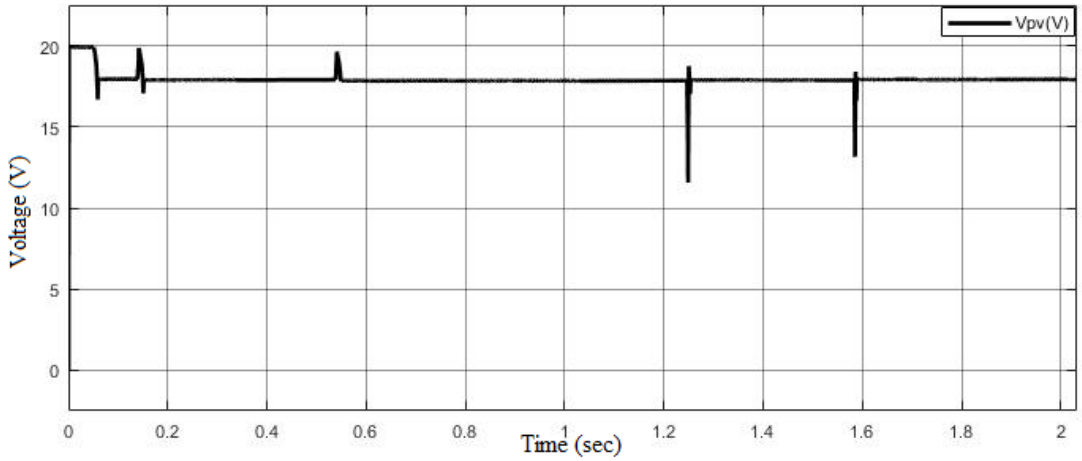

Figure 5.28. PV voltage for the IC algorithm.

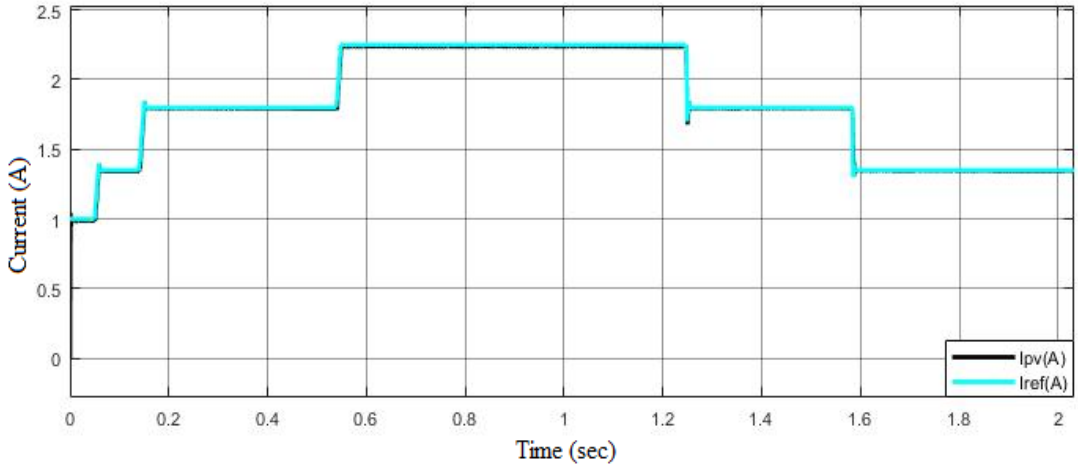

Figure 5.29. PV current and reference current for the IC algorithm.

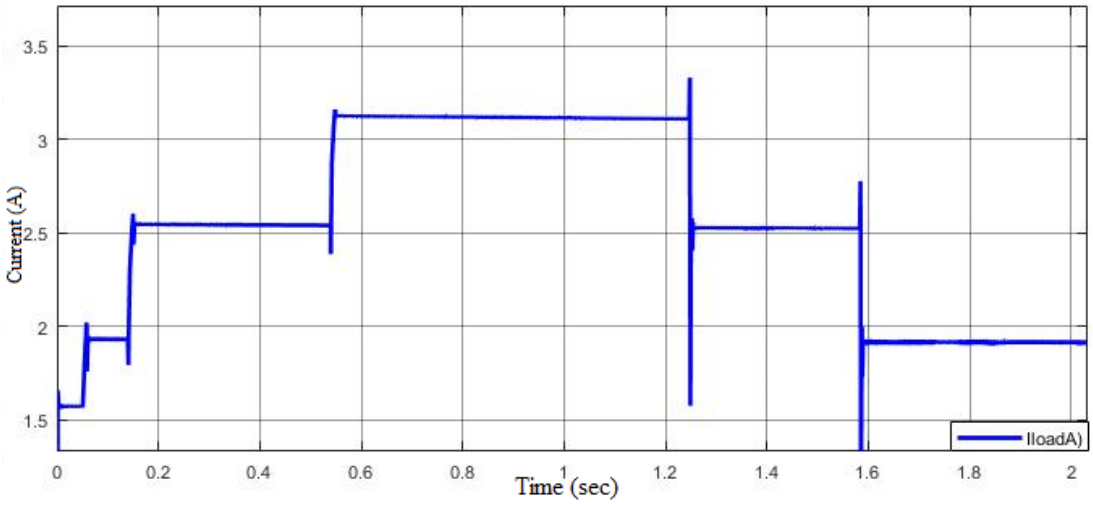

Figure 5.30. Load current for the IC algorithm.

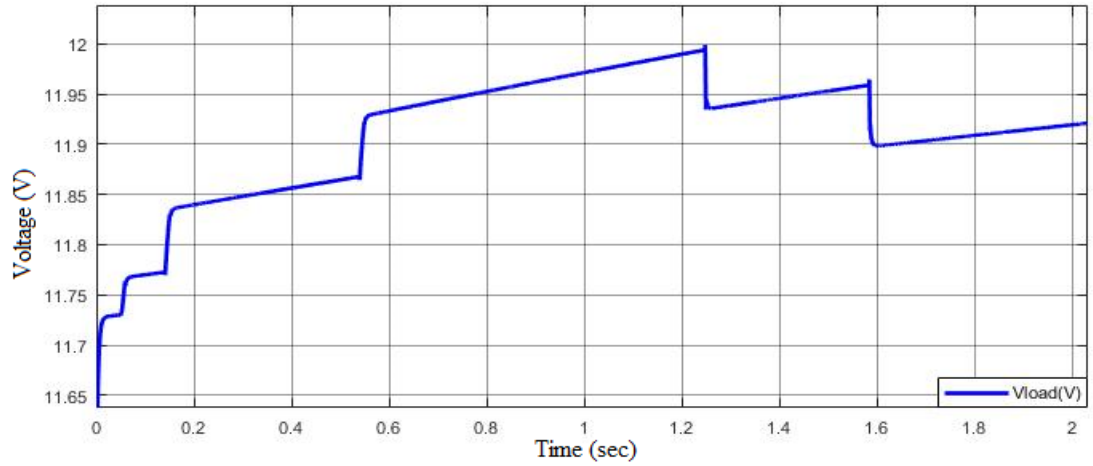

Figure 5.31. Load voltage for the IC algorithm.

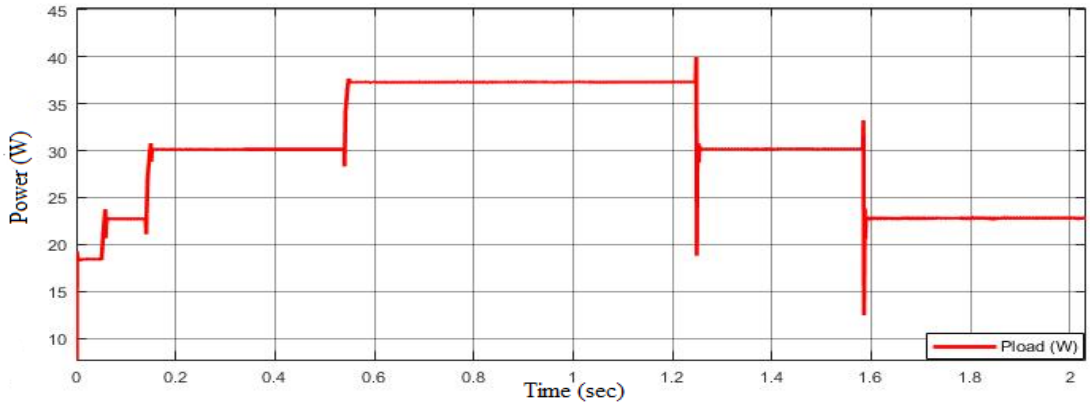

Figure 5.32. Load power for the IC algorithm**.**

Table 5.5. At the IC technique , the load power,voltage and PV power is measured at diffrent (SOC%) levels.

State of charge	**Irradiation (W/ m^2)**								
	600	800	1000	600	800	1000	600	800	1000
	P_{ext} (W)			**Pload(W)**			**Vbattery(V)**		
30	24.09	32.06	39.09	22.07	29.47	36.64	11.76	11.82	11.90
50	24.08	32.07	39.03	22.85	29.46	37.26	12.16	12.27	12.35
80	24.07	31.96	39.07	22.97	29.95	37.48	12.59	12.74	12.92
90	24.08	31.97	39.91	23.03	30.95	37.69	12.81	13.01	13.24

To enable complete and safe LA battery charging for the IC algorithm and achieve the result as shown in Table 5.5. The battery voltage is between 11.7V-11.9V when the SOC is at 30% capacity, which is increased to 12.35V at 50% SOC and than at 80% which is about 12.5V-12.9V, and reaches to 13.24V for the 90% SOC. According to result, it was clear that the SOC% increased, the battery voltage charge increased as well. Both the PV power and load power graphic are shown in Figure 5.33, Figure 5.34, Figure 5.35, and Figure 5.36 when the SOC is 30%, 50%, 80%, and 90% for the IC algorithm.

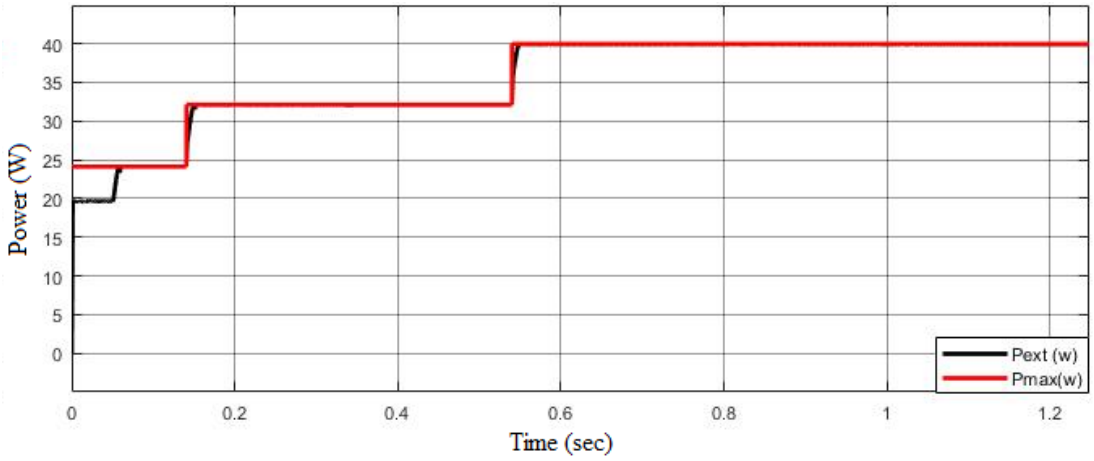

(a)

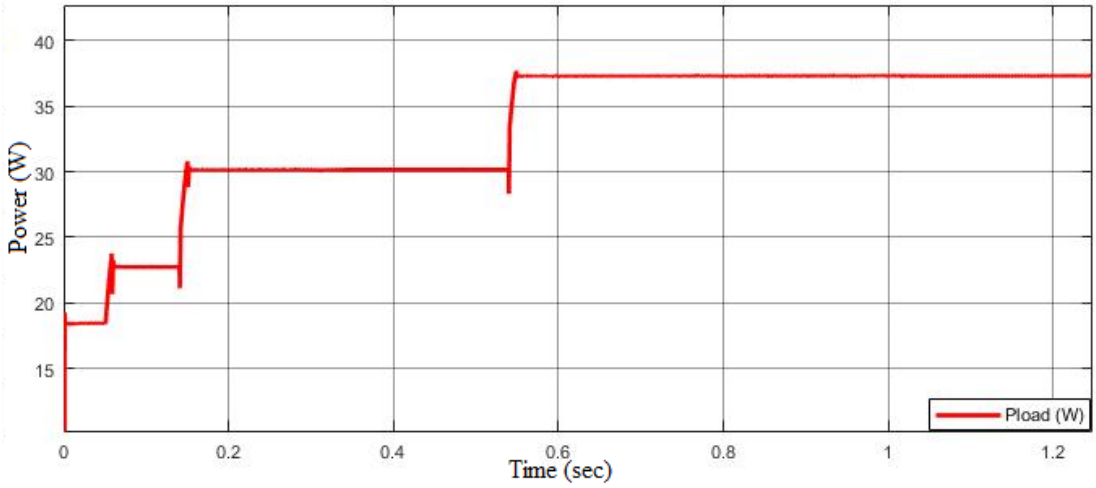

(b)

Figure 5.33. (30%) battery charge capacity graphic of (a) PV power, (b) Battery power**.**

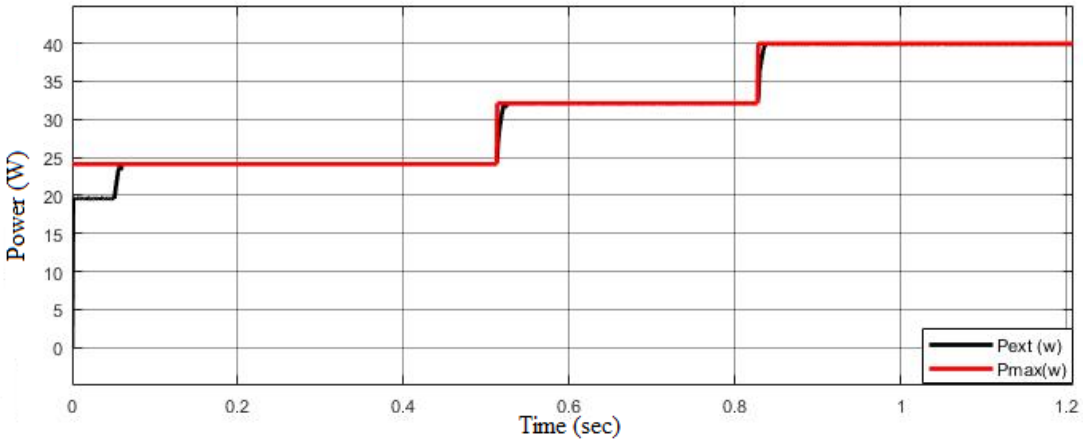

(a)

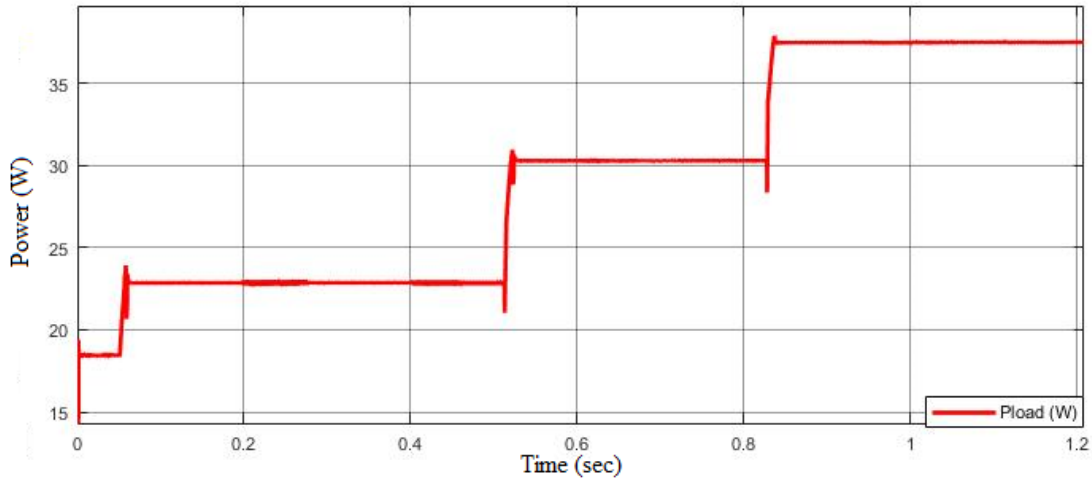

(b)

Figure 5.34. (50%) battery charge capacity graphic of (a) PV power, (b) Battery power.

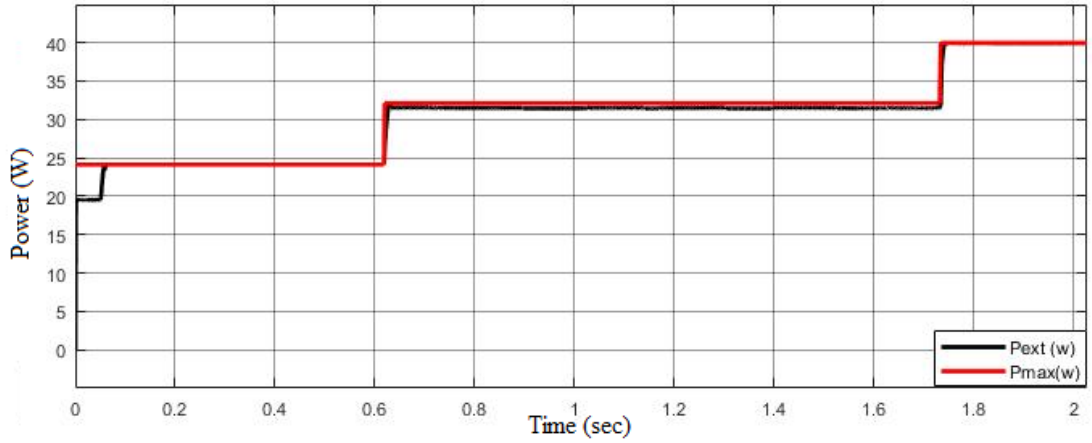

(a)

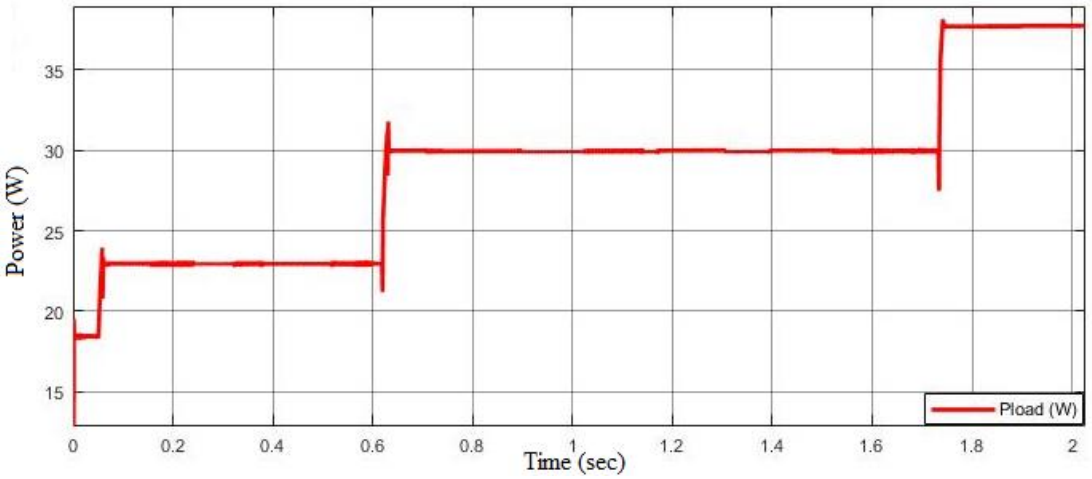

(b)

Figure 5.35. (80%) battery charge capacity graphic of (a) PV power, (b) Battery power**.**

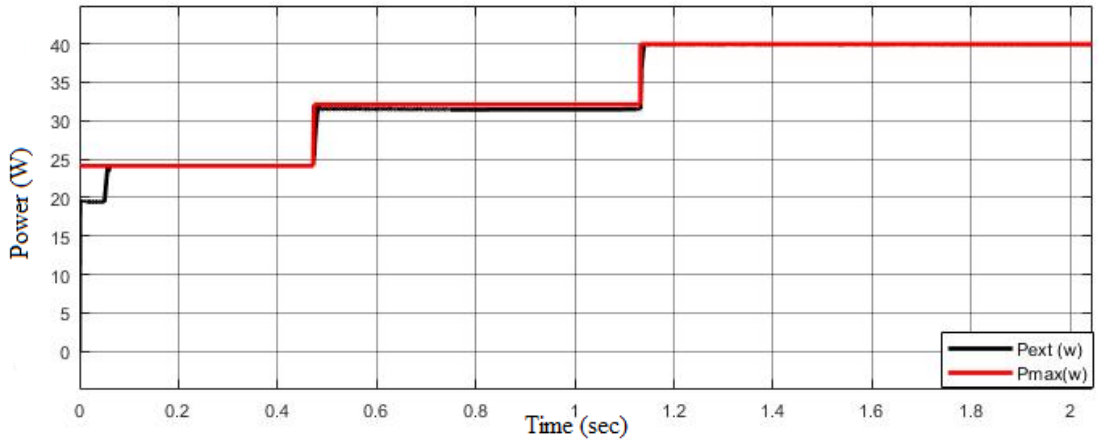

(a)

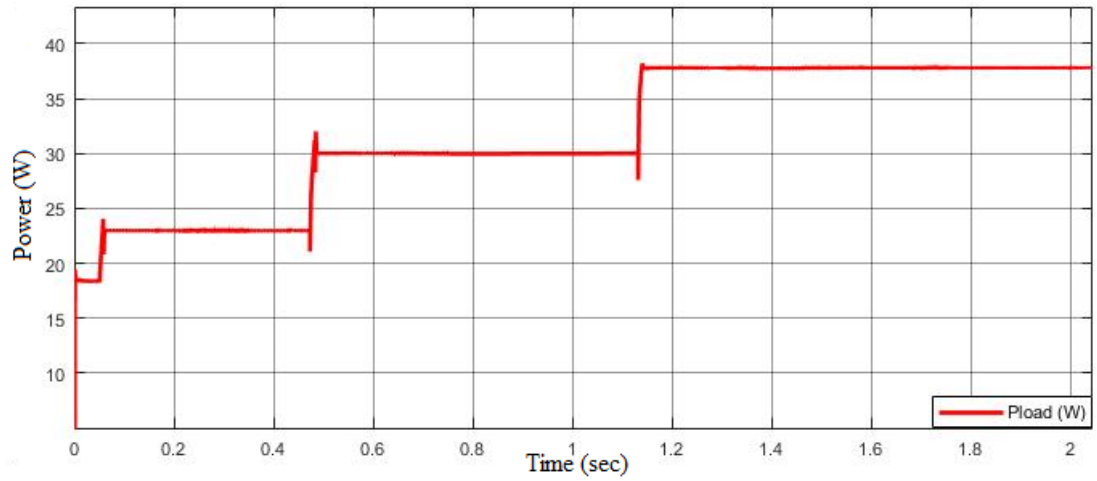

(b)

Figure 5.36. (90%) battery charge capacity graphic of (a) PV power, (b) Battery power.

The efficiency of the P&O and the IC algorithms at 600W/m^2 are about 99.79%. When the irradiation is increased to 800W/ m^2 the both algorithm have the same efficiency about 99.87% and when the radiation is increased to 1000 W/m^2 the IC has higher efficiency compared to the P&O algorithm and, then it was keep to be higher at changed to 800 W/m^2 than appears to have a similar efficiency at changed the radiation to 600W/ m^2, as shown in Table 5.6.

The efficiency is calculated for both the P&O and the IC algorithms as

$$\eta_{MPO} = \frac{Pext}{Pmax} \quad (5.1)$$

$$\eta_{MIC} = \frac{Pext}{Pmax} \quad (5.2)$$

where the η_{MPO} is the MP&O efficiency and η_{MIC} is the MIC algorithm efficiency and P_{ext} is the extracted PV power system pulled by the both algorithm and P_{max} is the maximum ideal power of the PV system.

Table 5.6. A comparison of the approaches used for P_{ext} and P_{max}.

	Irradiation (W/m^2)									
	600		800		1000		800		600	
	P&O	**IC**	**P&O**	**IC**	**P&O**	**IC**	**P&O**	**IC**	**P&O**	**IC**
P_{ext}	24.07	24.07	32.07	32.07	39.92	39.58	32.01	32.07	24.09	24.09
P_{max}	24.12	24.12	32.11	32.11	39.96	39.96	32.11	32.11	24.12	24.12
η%	99.79	99.79	99.87	99.87	99.85	99.89	99.68	99.87	99.87	99.87

PART 6

CONCLUSION

Renewable energy's role is being increasingly recognized, and its use for power generation has increasingly essential in recent years. PV systems are a renewable energy source that is becoming increasingly popular by becoming a promising alternative source due to its abundance, pollution free, and renewability. The battery plays a crucial role in storing the energy from the PV system, especially for autonomous systems. In this thesis, a PV battery charging system that can provide MPPT has been studied. P&O and IC methods widely used in the literature are adapted to the system, and the results are presented comparatively. Performance criteria such as steady-state error and convergence time are used for comparison.

It can be concluded from the results of this thesis that a variable step-size method may be applied to improve the MPPT performance.

REFERENCES

1. S. R. Sinsel, R. L. Riemke, and V. H. Hoffmann, “Challenges and solution technologies for the integration of variable renewable energy sources—a review,” ***Renew. Energy***, (145):2271–2285 (2020).
2. S. Sumathi, L. Ashok Kumar, and P. Surekha, *Solar PV and Wind Energy Conversion Systems*. (2015).
3. S. Padhee, U. C. Pati, and K. Mahapatra, “Design of photovoltaic MPPT based charger for lead-acid batteries,” ***2016 IEEE Int. Conf. Emerg. Technol. Innov.*** 351–356 (2016).
4. N. L. Panwar, S. C. Kaushik, and S. Kothari, “Role of renewable energy sources in environmental protection: A review,” ***Renew. Sustain. Energy Rev.*** (15) (3): 1513–1524 (2011).
5. H. A. SAMEEN, “Modelling And Performance Analysis Of Photovoltaic Systems In Kirkuk, Iraq,” (2017).
6. N. Belhaouas, M. S. A. Cheikh, A. Malek, and C. Larbes, “Matlab-Simulink of photovoltaic system based on a two-diode model simulator with shaded solar cells,” ***Rev. des Energies Renouvelables***, (16): 1–65 (2013).
7. M. Azzouzi, D. Popescu, and M. Bouchahdane, “Modeling of Electrical Characteristics of Photovoltaic Cell Considering Single-Diode Model,” ***J. Clean Energy Technol.***,(4) (6): 414–420 (2016).
8. E. Irmak and N. Güler, “A model predictive control-based hybrid MPPT method for boost converters,” ***Int. J. Electron.,***(107)(1): 1–16 (2020).
9. D. Dib, M. Mordjaoui, and G. Sihem, “Contribution to the performance of GPV systems by an efficient MPPT control,” ***Proc. 2015 IEEE Int. Renew. Sustain. Energy Conf. IRSEC 2015***,(2016).
10. X. Liu and L. A. C. Lopes, “An improved perturbation and observation maximum power point tracking algorithm for PV arrays,” ***PESC Rec. - IEEE Annu. Power Electron. Spec. Conf.***,(3): 2005–2010 (2004).
11. S.-I. Go, S.-J. Ahn, J.-H. Choi, W.-W. Jung, S.-Y. Yun, and I.-K. Song, “Simulation and Analysis of Existing MPPT Control Methods in a PV Generation System,” ***J. Int. Counc. Electr. Eng.***,(1)(4): 446–451 (2011).
12. H. S. H. Chung, K. K. Tse, S. Y. Ron Hui, C. M. Mok, and M. T. Ho, “A novel maximum power point tracking technique for solar panels using a SEPIC or Cuk converter,” ***IEEE Trans. Power Electron.***,(18) (3): 717–724 (2003).
13. S. Kolsi, H. Samet, and M. Ben Amar, “Design Analysis of DC-DC Converters Connected to a Photovoltaic Generator and Controlled by MPPT for Optimal Energy Transfer throughout a Clear Day,” ***J. Power Energy Eng.***, (02) (01): 27–34 (2014).
14. T. Esram and P. L. Chapman, “Comparison of photovoltaic array maximum power point tracking techniques,” ***IEEE Trans. Energy Convers.***,(22) (2): 439–449 (2007).

15. G. Remy, O. Bethoux, C. Marchand, and H. Dogan, “Review of MPPT Techniques for Photovoltaic Systems,” (2009).
16. F. J. A. MADI, “Maximum Power Point Tracking Using Firefly Algorithm For Solar Photovoltaic Systems,” no. December, (2018).
17. N. Femia, G. Petrone, G. Spagnuolo, and M. Vitelli, *Power Electronics and Control Techniques for Maximum Energy Harvesting in Photovoltaic Systems*. 2017.
18. J. S. Kumari, D. C. S. Babu, and A. K. Babu, “Design and analysis of P&O and IP&O MPPT techniques for photovoltaic system,” ***Int. J. Mod. Eng. Res.***, (2) (4): 2174–2180 (2012).
19. D. Choudhary and A. R. Saxena, “DC-DC Buck-Converter for MPPT of PV System,” ***Int. J. Emerg. Technol. Adv. Eng.***,(4): 7-9 (2014).
20. I. A. ADEN, “Design And Implementation Of Single Input Multiple Output (Simo) Dc-Dc Buck Converter For Solar Energy Application,” no. June, 2018.
21. R. W. Erickson and D. Maksimovic, *Fundamentals of Power Electronics*, Second edi. .
22. J. López, S. I. Seleme, P. F. Donoso, L. M. F. Morais, P. C. Cortizo, and M. A. Severo, “Digital control strategy for a buck converter operating as a battery charger for stand-alone photovoltaic systems,” ***Sol. Energy***, (2016)..
23. H. Lund, “Renewable energy strategies for sustainable development,” ***Energy***, (32) (6): 912–919 (2007).
24. D. E. Janzen and K. R. Mann, “Comprehensive Approach to Modeling and Simulation of Photovoltaic Arrays,” ***Dalt. Trans.***, (44) (9): 4223–4237 (2015).
25. L. Shengqing, L. Fujun, Z. Jian, C. Wen, and Z. Donghui, “An improved MPPT control strategy based on incremental conductance method,” ***Soft Computing***, (24) (8): 6039–6046 (2020).
26. N. Kumari, “International Journal of Computer Science and Mobile Computing Comparison of ANNs, Fuzzy Logic and Neuro-Fuzzy Integrated Approach for Diagnosis of Coronary Heart Disease: A Survey,” ***Ijcsmc***,(2) (6): 216–224 (2013).
27. A. L. dos S. Pereira, “Universal Programmable Battery Charger With Optional Battery Management System,” ***Ekp***, (13) (3): 1576–1580 (2015).
28. V. Regulated and L. Acid, “Bateria Chumbo-Ácida Selada Regulada por Válvula Valve Regulated Lead Acid Battery.”
29. A. F. Murtaza, H. A. Sher, M. Chiaberge, D. Boero, M. De Giuseppe, and K. E. Addoweesh, “Comparative analysis of maximum power point tracking techniques for PV applications,” ***2013 16th Int. Multi Top. Conf. INMIC 2013***, 83–88 (2013).
30. C. Boman, “Embedded impedance based state-of-charge estimation,” (2014).
31. K. Hirech, M. Melhaoui, F. Yaden, E. Baghaz, and K. Kassmi, “Design and realization of an autonomous system equipped with a charge/dischargeregulatorand digital MPPT command,” ***Energy Procedia***, (42): 503–512 (2013).
32. I. Yazlcl, E. K. Yaylacl, B. Cevher, F. Yalçln, and C. Yüzkollar, “A new MPPT method based on a modified Fibonacci search algorithm for wind energy conversion systems,” ***J. Renew. Sustain. Energy***, (13)(1): 0–1 (2021).

RESUME

Afnan Waleed A. SAFFAR she completed her primary and secondary education in Kirkuk. She holds a bachelor's degree in Electrical Engineering from the University of Kirkuk-College of Engineering, which she graduated in 2017.

e-mail: afnanwaleed95@gmail.com